

Summer 8-31-2001

## High solid loading aqueous base metal/ceramic feedstock for injection molding

Mohammad Behi  
*New Jersey Institute of Technology*

Follow this and additional works at: <https://digitalcommons.njit.edu/dissertations>



Part of the [Materials Science and Engineering Commons](#)

---

### Recommended Citation

Behi, Mohammad, "High solid loading aqueous base metal/ceramic feedstock for injection molding" (2001). *Dissertations*. 509.  
<https://digitalcommons.njit.edu/dissertations/509>

This Dissertation is brought to you for free and open access by the Electronic Theses and Dissertations at Digital Commons @ NJIT. It has been accepted for inclusion in Dissertations by an authorized administrator of Digital Commons @ NJIT. For more information, please contact [digitalcommons@njit.edu](mailto:digitalcommons@njit.edu).

## Copyright Warning & Restrictions

The copyright law of the United States (Title 17, United States Code) governs the making of photocopies or other reproductions of copyrighted material.

Under certain conditions specified in the law, libraries and archives are authorized to furnish a photocopy or other reproduction. One of these specified conditions is that the photocopy or reproduction is not to be “used for any purpose other than private study, scholarship, or research.” If a user makes a request for, or later uses, a photocopy or reproduction for purposes in excess of “fair use” that user may be liable for copyright infringement,

This institution reserves the right to refuse to accept a copying order if, in its judgment, fulfillment of the order would involve violation of copyright law.

**Please Note: The author retains the copyright while the New Jersey Institute of Technology reserves the right to distribute this thesis or dissertation**

Printing note: If you do not wish to print this page, then select “Pages from: first page # to: last page #” on the print dialog screen

The Van Houten library has removed some of the personal information and all signatures from the approval page and biographical sketches of theses and dissertations in order to protect the identity of NJIT graduates and faculty.

## **ABSTRACT**

### **HIGH SOLID LOADING AQUEOUS BASE METAL/CERAMIC FEEDSTOCK FOR INJECTION MOLDING**

by

**Mohammad Behi**

Increasing volume fraction of metal powder in feedstock provided lower shrinkage. Reduction of the shrinkage results in better dimensional precision. The rheology of the feedstock material plays an important role to allowing larger volume fractions of the metal powder to be incorporated in the feedstock formulations. The viscosity of the feedstock mainly depends on the binder viscosity, powder volume fraction and characteristics of metal powder.

Aqueous polysaccharide agar was used as a baseline binder system for this study. The effect of several gel-strengthening additives on 1.5wt% and 2wt% agar gel was evaluated. A new gel-strengthening additive was found to be the most effective among the others. The effect of other additives such as glucose, sucrose and fructose on viscosity of baseline binder and feedstock was investigated. Two new agar based binder compositions were developed. The use of these new binder formulations significantly improved the volume fraction of the metal powder, the stability of the feedstock, and reduced the final shrinkage of the molded articles. Two types of 17-4PH stainless steel metal powders, one gas atomized and, the other water atomized, were used for this research.

**HIGH SOLID LOADING AQUEOUS BASE METAL/CERAMIC FEEDSTOCK  
FOR INJECTION MOLDING**

**by  
Mohammad Behi**

**A Dissertation  
Submitted to the Faculty of  
New Jersey Institute of Technology  
In Partial Fulfillment of the Requirement for the Degree of  
Doctor of Philosophy**

**Department of Materials Science and Engineering**

**August 2001**

Copyright © 2001 by Mohammad Behi

ALL RIGHTS RESERVED

**APPROVAL PAGE**

**HIGH SOLID LOADING AQUEOUS BASE METAL/CERAMIC FEEDSTOCK  
FOR INJECTION MOLDING**

**Mohammad Behi**

~~Dr. Ken K. Chin, Dissertation Advisor~~ Date  
~~Professor of Physics and Director for the joint NJIT-Rutgers (Newark)~~  
~~Applied Physics Program and Director for Materials Science and~~  
~~Engineering Program, NJIT~~

~~Dr. Roland A. Levy, Committee Member~~ Date  
~~Distinguished Professor of Physics, NJIT~~

~~Dr. Ahmad Safari, Committee Member~~ Date  
~~Distinguished Professor of Ceramics and Materials Engineering,~~  
~~And member of the Center for Ceramics Research at Rutgers, The~~  
~~State University of New Jersey~~

~~Dr. Jerry C. LaSalle, Committee Member~~ Date  
~~Metal Injection Molding (MIM) Operations Director at~~  
~~Polymer Technologies Inc. in Clifton, New Jersey~~

~~Dr. Liang Xue, Committee Member~~ Date  
~~Research Scientist at Honeywell International in Morristown, New Jersey~~

## BIOGRAPHICAL SKETCH

**Author:** Mohammad Behi  
**Degree:** Doctor of Philosophy  
**Date:** August 2001

### **Undergraduate and Graduate Education:**

- Doctor of Philosophy in Materials Science and Engineering  
New Jersey Institute of Technology, Newark, NJ, 2001
- Master of Science in Materials Science and Engineering  
Stevens Institute of Technology, Hoboken, NJ, 1986
- Bachelor of Science in Metallurgy  
Western Michigan University, Kalamazoo, MI, 1982

**Major:** Material Science and Engineering

### **Publications and Patents:**

Mohammad Behi, Ken Chin and Jerry LaSalle

“Gel-strengthening additives for agar based binder system for metal and ceramic injection molding feedstock”

Proceedings of the May 2001 MPIF Conference on Powder Metals, New Orleans, Louisiana

James Stevenson, Mohammad Behi, Jerry LaSalle,

“Recycle, Dry Feedstock, and Shrinkage Control Capabilities for MIM Compounds with Aqueous-Gel Binders”

Proceedings of the May 2001 MPIF Conference on Powder Metals, New Orleans, Louisiana

Mohammad Behi, M. Maxfield,

“Superconducting Ceramics By Sequential Electro-deposition”, Patent 5,162,295, 1992.

Anthony Fanelli, Mohammad Behi,  
“Gel Strength Enhancing Additives for Agaroid-Based Binder”, Patent 5,746,957,  
1998.

Mohammad Behi, Chien Wei Li, Jean Yamanis,  
“Silicon Nitride Body Having High As-Fired Surface Strength”, Patent WO  
96/32359, October 1996.

Mohammad Behi, Anthony Fanelli,  
“Aluminum Oxide-Based Molding Compound for Injection Molding”, Filed.

Mohammad Behi, Anthony Fanelli, Joan Burlew,  
“Process for Forming an Article from Recycled Ceramic Molding Compound”,  
Patent 6,146,560, November 2000.

Mohammad Behi, Jerry LaSalle, George Glandez,  
“Stable Aqueous Iron Based Feedstock Formulation for Injection Molding”,  
Patent 6,261,336, July 2001.

Jim Schoonover, Mohammad Behi, Michael Zedalis,  
“Low Pressure Injection Molding of Metal and Ceramic Powders Using Soft  
Tooling”, Patent 6,203,734, 1999.

Mohammad Behi, Anthony Fanelli,  
“Aqueous Injection Molding Binder Composition and Molding Process”, Patent  
6,262,150, July 2001.

Mohammad Behi, Joan Burlew,  
“Improving of Flow Characteristics of Stainless Steel Metal Feedstock for  
Injection Molding”, Filed.

Chien Wei Li, Mohammad Behi, Jean Yamanis,  
“Super-Tough Monolithic Silicon Nitride Ceramic”, Patent 5,100,647, 1992.

Mohammad Behi, Richard Duyckinck, Michael Zedalis,  
“Metal/Ceramic Composite Molding Material for Injection Molding”, Patent  
6,291,560, September 2001.

Mohammad Behi, Jim Schoonover, Michael Zedalis,  
“Rapid Manufacturing of Metal and Ceramic Tooling”, Patent 6,056,915, 2000.

Mohammad Behi, Malanie Matic, Chien Wei Li,  
“Aqueous Coarse Silicon Carbide Feedstock for Injection Molding”, Filed.

James Stevenson, Mohammad Behi, Jerry LaSalle, Gary Marsh,  
“Recycle Methods for Water Based Powder Injection Molding Compound”, Filed.

Charles Gasdaska, Mohammad Behi, Vikram Jamalabad,  
“Freeform Manufacture of Structural Metal and Ceramic Components Using  
Aqueous Binders”, Filed.

Mohammad Behi, Joan Burlew, Jerry LaSalle,  
“Aqueous Nonferrous Feedstock Material for Injection Molding”, Filed.

Mohammad Behi, Richard Duyckinck, Anthony Fanelli,  
“Aqueous Injection Molding Binder Composition and Molding Process”, Patent  
6,262,150, 2001.

Chien Wei Li, Mohammad Behi, Jean Yamanis,  
“Monolithic Silicon Nitride Ceramic Having High Fracture Toughness”, Patent  
5,449,649, 1995.

*In the Name of God, the Most Gracious, the Most Merciful*



To my wife Pari for her continuous support and encouragement  
and my daughter Mona and my sons Mazzi and Sajjad for their patience

## **ACKNOWLEDGMENT**

Sincerest thanks to Dr. Ken Chin my Thesis Advisor for the professional advice, guidance, direction, and moral support that has made this project possible. Special thanks to my committee members Dr. L. Levy and Dr. A. Safari for reviewing my thesis.

My special thanks to Dr. Liang Xue and Dr. Jerry LaSalle for their comments, rendered invaluable assistance in reviewing and fine tuning of my research and data analysis. Their availability and time-consuming efforts are very much appreciated.

My thanks are extended to AlliedSignal-Honeywell Corporation for their facilities and supports in completing this project. Also, my thanks go to Dr. Tony Fanelli, and Dr. James Stevenson for their comments and suggestions throughout this study. I extend my thanks to Joan Burlew, Richard Roser, George Glandez, Craig Scott, Brian Snow, Steve Sesny, and Bill Fisher for their assistance in this research.

Last, but not least I would like to thank my wife Pari for her continuous support and encouragement for this and all the other aspects in my life, also, thank to my daughter Mona, my sons Mazzi and Sajjad for their patience and understanding for so many years.

## TABLE OF CONTENTS

Chapter	Page
1 INTRODUCTION.....	1
2 BACKGROUND INFORMATION.....	5
3 STUDY OF THE VARIOUS ASPACTS OF POWDER SELECTION FOR MIM PROCESS.....	8
3.1 Effect of Particle Size Distribution.....	8
3.2 Type of Powders .....	14
3.3 Stability of Metal Powders in Aqueous Media .....	16
4 THE AQUEOUS BINDER.....	18
4.1 Agar Binder.....	18
4.2 Viscosity of Agar Gel.....	20
4.3 Study of the Gel Strength of Agar Binder.....	21
4.4 Experimental Procedure.....	22
5 BINDER ADDITIVES.....	26
5.1 Effect of Additives on Gel Puncture Strength of Agar .....	26
5.2 New Gel-Strengthening Additive.....	27
6 THE AQUEOUS BASELINE METAL FEEDSTOCK.....	32
6.1 Baseline Formulation .....	32
6.2 Experimental Batch Using Water Atomized Powder .....	33
6.3 Flow Characteristics of Baseline Formulation.....	36
6.4 Spiral Flow Mold .....	36
6.5 Experimental Procedure.....	39
6.6 Results.....	40

**TABLE OF CONTENTS**  
**(Continued)**

<b>Chapter</b>	<b>Page</b>
6.7 Experimental Batch Using Gas-atomized Powder.....	43
6.8 Experimental Procedures .....	43
6.9 Results.....	44
7 BINDER SYSTEM COMPONENTS.....	47
7.1 Effect of Binder System Components on Density of the Feedstock .....	47
7.2 Effect of Additives on Rheology of 17-4PH Feedstock.....	50
7.3 Experimental Procedures .....	51
8 THE FLOW PROPERTIES OF AGAR-GLUCOSE COMPOSITIONS.....	52
8.1 Flowability of Composition “A”.....	52
8.2 Flowability of Composition “B”.....	52
8.3 Flowability of Composition “C”.....	53
8.4 Flowability of Composition “D”.....	53
8.5 Flowability of Composition “E”.....	54
8.6 Flowability of Composition “F”.....	54
8.7 Flowability of Composition “G”.....	54
8.8 Results and Discussion .....	55
8.9 Effect of Solid Loading on Molding Weight .....	58
9 FEEDSTOCK CONTAINING 17-4PH ATMIX POWDERS.....	61
9.1 Study the Effect of Additives on 17-4PH (Atmix) Feedstock.....	61
9.2 Glucose Additives.....	61
9.3 Sucrose Additives .....	62

**TABLE OF CONTENTS**  
**(Continued)**

<b>Chapter</b>	<b>Page</b>
9.4 Fructose Additives .....	63
9.5 Results and Discussion .....	63
9.6 Effect of Solid Loading on As-Molded Weight.....	65
9.7 Composition “A” Containing 17-4PH (Atmix) Powder .....	68
9.8 Results and Discussion .....	70
10 THE SINTERING PROCESS .....	72
10.1 Debinding.....	72
10.2 Sintering.....	73
10.3 Shrinkage Prediction and Measurements.....	77
11 CONCLUSIONS.....	82
11.1 Concluding Remarks.....	82
11.2 Future Research.....	84
REFERENCES .....	85

## LIST OF TABLES

Table	Page
1.1 Various binder systems .....	4
2.1 Nominal composition of precipitation hardening wrought stainless steel .....	6
3.1 Effect of particle size distribution on tap density.....	11
3.2 Typical chemical composition of 17-4PH powder.....	15
4.1 Official specification of agar.....	20
4.2 Effect of agar (TIC100) concentration on gel strength.....	25
5.1 Effect of borate compounds on puncture strength of agar gels .....	27
5.2 Effect of potassium tetraborate on gel strength of 1.5wt% agar Concentration .....	29
5.3 Comparison effect of different additives on gel strength of 2wt% agar gel...	30
6.1 Machine setting for spiral flow testing.....	39
8.1 Summary of flow characteristics of agar-glucose feedstock composition for 17-4PH (UFP) gas atomized powder .....	56
9.1 Summary of the molding results for 17-4 PH (Atmix) composition “G <sub>w</sub> ” ....	67
9.2 Summary of the molding results for 17-4 PH (Atmix) composition “A <sub>w</sub> ” ....	69
9.3 Summary and results of agar-glucose formulations for 17-4PH (Atmix) water-atomized powder .....	71
10.1 The effect of feedstock formulation on shrinkage.....	79
10.2 Carbon and oxygen content of 17-4PH before and sintering .....	81

## LIST OF FIGURES

<b>Figure</b>	<b>Page</b>
2.1 Schematic drawing of an injection end of reciprocating screw machine .....	7
3.1 SEM micrograph of powders (a) 17-4PH gas atomized (UFP), (b) 17-4PH water-atomized (Atmix) and (c) 17-4PH gas atomized (Anval) powders .....	12
3.2 Tap densities vs. mixing ratio of powder with different particle sizes .....	13
3.3 Stability of various metal powders in aqueous environment .....	17
4.1 Effect of temperature on viscosity of agar (agar 100 from Meer Inc.).....	21
4.2 Puncture apparatus .....	23
4.3 Effect of agar (TIC100) concentration on gel strength.....	24
5.1 Effect of potassium tetraborate on gel strength of 1.5wt% agar gel.....	28
5.2 Effect of potassium tetraborate on gel strength of 2wt% agar gel.....	30
6.1 Schematic of (a) Hobart shredder, (b) Arizona moisture analyzer.....	35
6.2 (a) “A” and “B” sides of the spiral mold (b) spiral mold cavity .....	38
6.3 Effect of injection molding pressure on flowability of 17-4PH (Atmix) baseline compositions .....	41
6.4 Effect of solid loading on flowability of 17-4PH (Atmix) baseline compositions.....	42
6.5 Effect of injection molding pressure on flowability of 17-4PH (UFP) baseline compositions .....	45
6.6 Effect of solid loading on flowability of 17-4PH (UFP) baseline compositions.....	46
7.1 Effect of agar content on density of stainless steel 17-4PH feedstock.....	48
7.2 Effect of moisture content on feedstock density containing 2wt% agar .....	49
8.1 Shows the tensile bar mold and the cavity dimensions of the mold.....	59

**LIST OF FIGURES**  
**(Continued)**

<b>Figure</b>	<b>Page</b>
8.2 Effect of solid loading of 17-4PH (UFP) materials on molded weights of tensile bar samples .....	60
9.1 Effect of different additives on flowability of 17-4PH (Atmix) feedstock ....	65
9.2 Weight variation of as-molded parts using 17-4PH (Atmix) feedstock containing glucose additive (composition “G <sub>w</sub> ”) .....	67
9.3 Weight variation of as-molded parts using 17-4PH (Atmix) feedstock containing glucose additive (composition “A <sub>w</sub> ”) .....	69
10.1 Alternative paths for matter transport during the initial stages of sintering...	74
10.2 Change of pore shape and dimensional changes during sintering process.....	75
10.3 Influence of the sintering temperature and sintering time on liner shrinkage	76
10.4 Shrinkage model prediction and data for 17-4PH composition .....	78

## CHAPTER 1

### INTRODUCTION

Conventional injection molding is one of the most common forming processes for polymers that melt on heating. This process is probably the most interesting method for mass production of small, medium and large sized parts having complex geometries. This method, which is well known for producing plastic parts, was adopted for oxide ceramics in the mid-thirties [1]. This process also has been implemented to develop a new technology known as Powder Injection Molding (PIM), which is applicable to forming (shaping) metal and ceramics articles. A subset of PIM is Metal Injection Molding (MIM). This process emerged in the 1980's as a manufacturing process to form complex and near-net shape components.

The feedstock material for this process is a combination of 35-50 vol% of binder with metal, ceramic or mixture of both powders [2] that can be molded in simple or complicated shapes using conventional injection molding machines. The attributes of the binder are crucial for successful MIM production. It is not only a necessary aid for viscous flow of the powder into the mold but should also ensure stability of the green part [3]. A variety of different low molecular weight polymer material such as polyethylene glycol (PEG), polyethylene (PE), polystyrene (PS), paraffin wax (PW), polyethylene carbonate (PEC), and polyvinyl chloride (PVC) are among the common binders used for PIM process. In general, thermoplastic and thermosetting compounds are two forms of polymers that are used in PIM. The viscosity of thermoplastic polymer is thermally reversible. Their viscosity decreases upon heating and increases (hardens) on cooling.

The process is independent of the number of cycles. The thermosetting polymers are not thermally reversible. They permanently form cross-links upon heating. The thermosetting polymers do not soften on re-heating but decompose at elevated temperature. Candle wax and polyurethane are two examples of these two forms of polymers. The melting temperature of low molecular weight thermoplastic polymers ranges from 60°C for paraffin wax to 140-200°C for polypropylene [1]. Many different binder compositions have been designed to be used for PIM process. Most of them are thermoplastic binders comprising of a mixture of wax and polymer. Chung [4] used a commercial polyethylene wax (PEW) as a binder system. Cao [5] selected a mixture of PEG with Phenoxy, PMMA and OPEW in his binder formulation. Anwar [6] [7] used a combination of three different grades of PEG with PMMA (polymethyl Methacrylate) for his study. A mixture of Polybutyl-methacrylate and Polystyrene was employed by Kankawa [8]. Table 1.1 illustrates several examples of PIM binder formulation and their compositional diversities.

The feedstock material is produce by incorporating the fine metal powders with the selected binder. The flow characteristics of the feedstock significantly are affected by the properties of binder system, metal powder/binder ratio, particle size, shape and particle size distribution of the metal powder and mixing techniques. Mechanical mixing is conducted at the melting temperature of the binder and followed by palletizing and molding the feedstock. Unlike the binder systems, limited information has been published in detail on techniques for preparation of feedstock. Libb and Patterson [9] used vacuum assisted sigma mixer to produce feedstock and evaluated the homogeneity and specific gravity of the feedstock.

Debinding is a critical step before sintering. At this step, the majority of the binder is extracted from molded parts by heat, solvent or combination of both. Every binder system has its own removal characteristics. In some systems, hot nitric acid vapors are used for debinding [10]. In others, an organic solvent is used. Frequently, a combination of plastic with waxes is used as binder systems to aid Debinding. The wax can melt and flow out of the part at a low temperature, leaving behind an interconnected network for brown strength and handleability prior to vaporization of the plastic during sintering cycle [9]. Difficulties associated with debinding impose a major barrier for PIM processes. Due to the extremely small sizes of powders, it is difficult to mix a binder with fine powders to form a mixture and, later in the production cycle, to take the binder out of the mixture [4]. A long debinding time from several hours to several days which is impractical in a manufacturing setting, is usually practiced to avoid any distortion or blowout of the green parts during debinding. The choice of debinding depends on the binder system. It could effects process economics, dimensional tolerance and wastes.

Sintering is a high temperature bonding and densification process taking place between the metal particles. It can occur by evaporation and condensation, liquid phase, or solid-state mechanism. Sintering is a diffusion process, which is effected by temperature, time, particle size and inter-particle space between the particles. It is conducted under inert gas or vacuum or combination of air, vacuum and inert gas. Various sintering schedules have been developed to generate maximum density for MIM parts, but the detail of the process generally is proprietary. Bloemacher [11] applied sintering temperature of 1300-1400°C for less than 2 hours to sinter 316-L tensile bars. He defined the detail of the sintering condition except the sintering atmosphere.

**Table 1.1** Various Binder Systems

Type of Binder	Binder Composition [1][6][7]
Thermoplastics	50% paraffin wax, 40% polypropylene, 10% camauba wax
	69% paraffin wax, 20% polypropylene, 10% camauba wax, 1% stearic acid
	67% polypropylene, 22% microcrystalline wax, 11% stearic acid
	33% paraffin wax, 33% polyethylene, 33% beeswax, 1% stearic acid
	65% polyethylene glycol, 30% polyvinyl butyryl, 5% stearic acid
	55% paraffin wax, 25% polyethylene glycol, 10% stearic acid, 10% dibutyl phthalate
	8% PEG <sub>800</sub> , 8% PEG <sub>1000</sub> , 64% PEG <sub>1500</sub> , 20% PMMA
Thermosetting	65% epoxy resin, 25% paraffin wax, 10% butyl stearate

## CHAPTER 2

### BACKGROUND INFORMATION

In general, the feedstock material is a mixture of one or more metal or ceramic or mixture of both powder and the binder used in shape forming processes such as injection molding. Various feedstock formulations based on different powders and binder formulation have been developed by others. Ideally, the feedstock should be designed to be stable with time, easy to mold and to have sufficient uniformity to provide dimensional control suitable for commercial application. Factors determining the attributes of the feedstock are, type of alloy powder, particle size and shape of the powder, chemical stability of the powder, binder composition, powder-binder ratio, moisture content and mixing method.

In this study, agar is used as the primary binder system and 17-4PH water and gas atomized stainless steel powders are used as a major component of the feedstock. The 17-4PH (Precipitation-Hardening) stainless steels alloy were developed during World War II as a new group of stainless steels with precipitation-hardening characteristics [12]. The first of these nonstandard grades of stainless steels, 17-4PH, was made available in 1948. The nominal chemical composition of some representative precipitation-hardening stainless steels is given in Table 2.1. In general, they have lower nickel content and may have elements such as copper or aluminum that tend to form coherent alloy precipitates. The feedstock comprises of metal powder, polysaccharide (Agar) binder and D.I H<sub>2</sub>O. Minor amount of two types of biocides (Methyl-p-hydroxybenzoate and propyl-p-hydroxybenzoate) are included in the feedstock formulation to prevent bacteria growth and deterioration of the agar with aging.

**Table 2.1** Nominal composition of precipitation hardening wrought stainless steel

Grads	%C	%Mn	%Si	%Cr	%Ni	%Mo	Others%
17-4 PH	0.04	0.04	0.5	16.50	4.25	.....	0.25 Cb, 3.60 Cu
17-4 PH	0.07	0.70	0.40	17.00	7.00	.....	1.15 Al
PH15-7 Mo	0.07	0.70	0.40	15.00	7.00	2.25	1.15 Al
17-10 P	0.12	0.75	0.50	17.00	10.50	.....	0.28 P

A 3000 cc Abbe sigma mixer is used for all the experimental batch preparation. The mixer is equipped with variable mixing speed up to 35 rpm maximum. The mixing temperature is controlled by a Cincinnati Milacron water heater, model MWC-75, with a temperature range of 1 to 121°C. A Hobart shredder is used to shred the feedstock to adequate sizes for ease feeding into an injection machine. A rotary pan drier designed and used to adjust the moisture content of the shredded feedstock material. A Boy 22M (22 tons) and a 55 tons Cincinnati injection molding machines were used for molding and evaluating different feedstock formulation. Figure 2.1 presents a schematic drawing of an injection end of reciprocating screw machine [13].

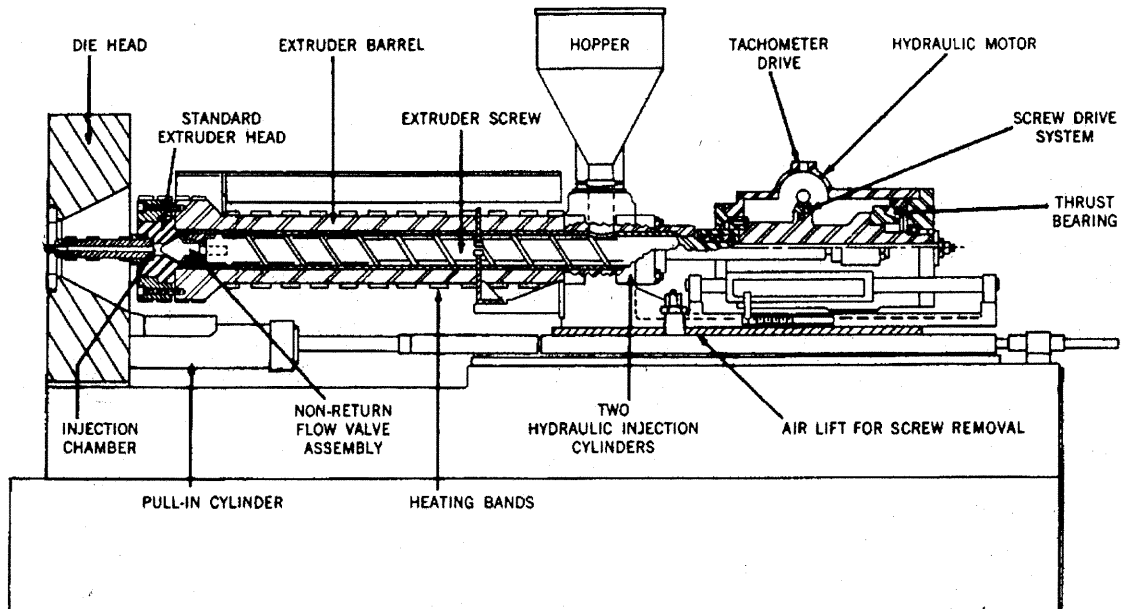


**Figure 2.1** Schematic drawing of an injection end of reciprocating screw machine.

## CHAPTER 3

### STUDY OF VARIOUS ASPECTS OF POWDER SELECTION FOR MIM PROCESS

#### 3.1 Effect of Particle Size Distribution

Powder characteristic is among one of the important factors affecting the rheology of the feedstock. Particle size distributions and particle shape, packing density, stability of the powder in an aqueous environment are the initial considerations for selecting a metal powder for a feedstock formulation. The attributes of an ideal powder has been reported by many researchers to have a particle size between 0.5 and 20  $\mu\text{m}$  with  $D_{50}$  between 4 to 8  $\mu\text{m}$ , tap density over 50% of theoretical density and particle size distribution of 2 or 8 ( $D_{90}/D_{10}=19$  or 2).

The particle size distribution number is calculated from the slope of the particle size distribution curve. Larger values correspond to narrower particle size distribution and small values indicate broad distribution. Non-agglomerated powder is highly preferred. When using aqueous Agar gel binder, at least two other requirements should be considered as critical requirements, stability of the powder in aqueous medium and specific surface area of the powder. As the specific surface area increases, the powder becomes less desirable to be used with Agar binder system. The powders with large surface area have a tendency to agglomerate and also require more binder (low solid loading) to produce a moldable feedstock. Concern with small particle size is inter-particle friction, which, adversely affects the powder flow and packing. The inter-particle friction in powder mass increases as the particle size decreases [14]. This type of powder generally requires more binder, and vigorous mixing, and thus creates feeding,

flowing, packing, and cracking problems during molding. On the other hand, a powder with low inter-particle friction creates problem with shape preservation during debinding and sintering. However, the desire for larger sized powder for molding must be balanced by the desire to have a small particle size to increase the green density and promote densification during the downstream sintering process.

The compacted angle of repose is used as a simple tool to compare and evaluate inter-particle friction of different powders [15]. The powder is compacted by vibration to high packing density. The angle of resistance to shear is measured by tilting the compacted powder from horizontal to cause shear. Large spherical particles will exhibit an angle of repose near 30° and it ranges up to 38° for free flowing powder [14]. When the angle of repose exceeds approximately 45°, the powder is termed cohesive.

The specific surface area of a powder can be calculated from the mean particle size  $\bar{a}_{V/A}$  [16] using the equation

$$S_m = \psi_A / \psi_V / \bar{a}_{V/A} D_a \quad (3.1)$$

A shape factor ratio  $\psi_A / \psi_V$  of 6 is usually assumed when the specific shape factors of the particles are unknown,  $\bar{a}_{V/A}$  ( $m^3/m^2$ ) is the average particle size of powder,  $D_a$  is apparent density of the powder. The specific surface area becomes more sensitive to variation in the shape and size of particles finer than 1  $\mu m$ .

$$S_m = 6 / \bar{a}_{V/A} D_a \quad (3.2)$$

The apparent surface area  $S_a$  of powder can be evaluated from equation 3.2 by using tap density  $\rho_{\text{tap}}$  and average particle size of powder  $D_{50}$ .

$$S_a = 6 / D_{50} \rho_{\text{tap}} \quad (3.3)$$

Higher  $\rho_{\text{tap}}$  associated with broader particle size distribution and higher spherically shaped powder. This indicates that powders with smaller average particle size and /or broader particle size distribution is not an ideal powder to be selected for MIM feedstock. To show the effect of broad particle size distribution on tap density, three different 17-4PH powders were evaluated. Two gas atomized and one water atomized 17-4PH powder were selected for this study. Table 3.1 shows the effects of particle size distributions on tap density for these powders. Figure 3.1 shows the SEM of the powders and their particle size and shape differences. The 17-4PH Anval gas atomized powder gained highest tap density of 61.7% of theoretical density. The water-atomized powder having irregular and semi-round particle shape was gained lowest tap density of 56.8%. The gas atomized UFP powder gained 57.8% of theoretical density.

**Table 3.1** Effects of particle size distribution on tap density

Type of Powder	Particle Size Distribution			D <sub>90</sub> /D <sub>10</sub>	Theoretical Density (g/cm <sup>3</sup> )	Tap Density (% T.D)
	D <sub>10</sub>	D <sub>50</sub>	D <sub>90</sub>			
	(μm)	(μm)	(μm)			
17-4PH (Gas)	4.85	12.11	21.59	4.45	7.78	4.50 (57.8)
17-4PH (Water)*	3.38	9.33	23.93	7.08	7.78	4.30 (55.3)
17-4PH (Gas)**	7.1	15.2	25	3.52	7.78	4.80 (61.7)

\*UFP gas atomized powder, \*\*Atmix water atomized powder, \*\*\*Anval gas atomized powder

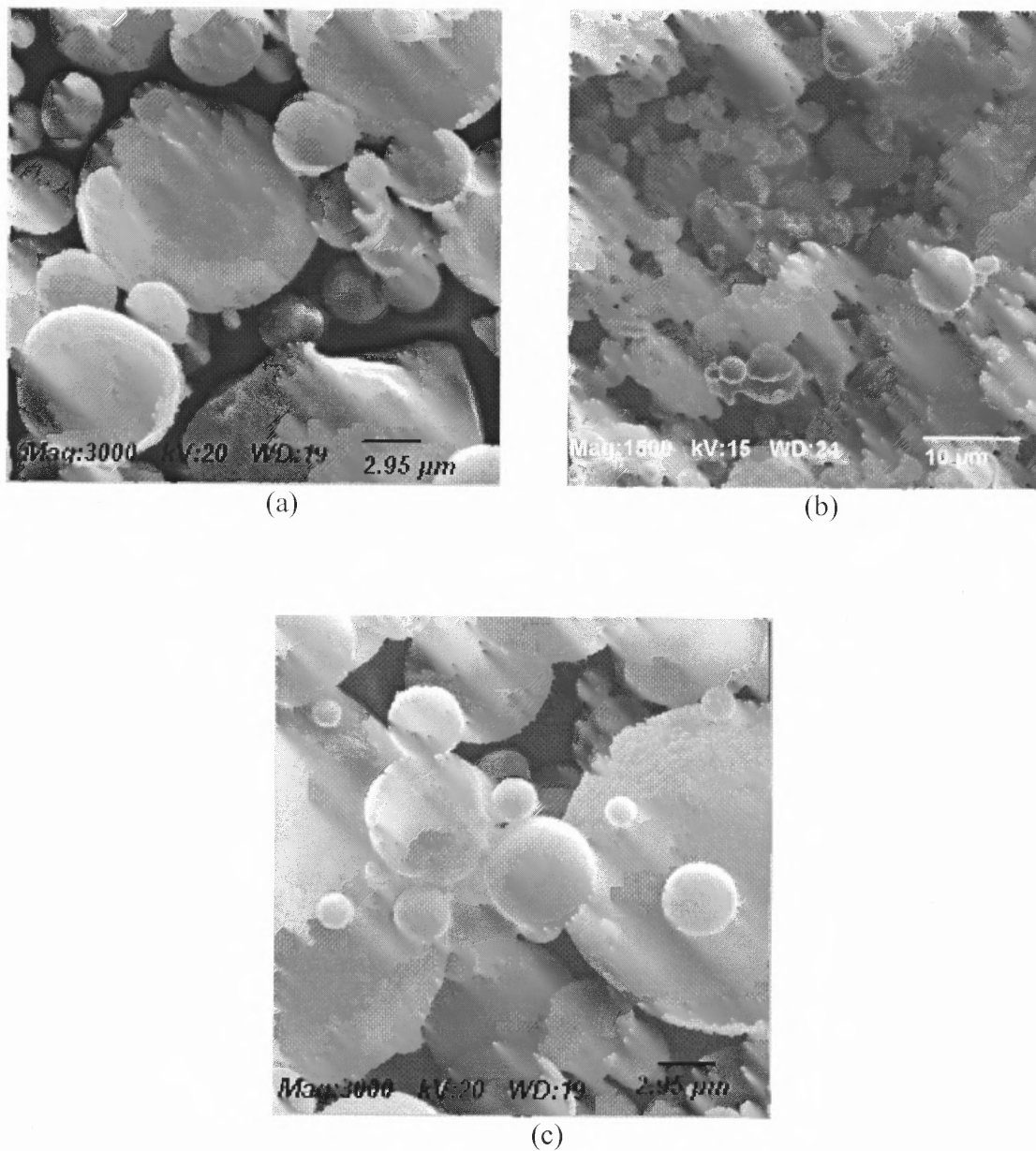


**Figure 3.1** SEM micrograph of the powders, a) 17-4PH gas-atomized UFP, b) 17-4PH water-atomized Atmix, and c) 17-4PH gas-atomized Anval powders

Large value for  $D_{90}/D_{10}$  correspond to narrow particle size distribution and small values indicates broad distribution. Data in Table 3.1 shows that the tap density increases for broader particle size distribution. The 17-4PH Anval powders, which have a lowest  $D_{90}/D_{10}$ , were gained highest 61.7% of theoretical density. The particle size distribution can be tailored to improve the tap density. The following experiment shows the effect of mixing ratio on tap density. Stainless steel gas atomized 316L Anval -53 and -22 microns powders were used for this experiment. The tap densities of five samples with 90:10, 80:20, 70:30, 60:40, and 50:50 ratio of -53:-22 micron powder were evaluated. Figure 3.2 shows the result of the experiment. The optimum ratio was determined to be at 60:40 ratios for this powder.

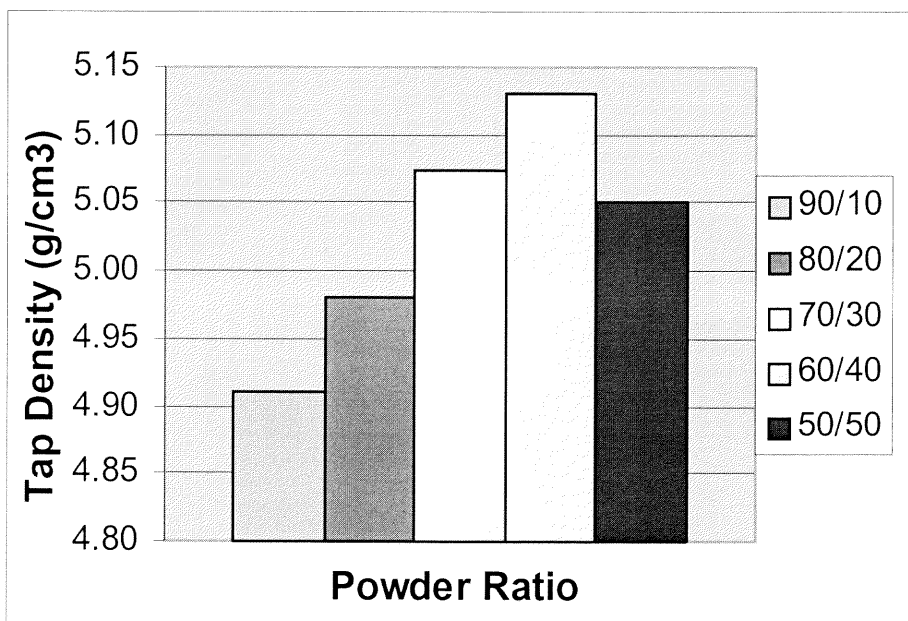


**Figure 3.2** Tap densities vs. mixing ratio of powder with different particle sizes.

The tendency of the powder to form voids between its particles can be evaluated by calculating the void volume from the tap density.

$$V_{\text{void}} = V_{\text{tap}} - V_{\text{true}} \quad (3.4)$$

$$V_{\text{void}} = m/\rho_{\text{tap}} - m/\rho_{\text{true}} \quad (3.5)$$

$V_{\text{void}}$  is volume of the void in  $\text{cm}^3$ ,  $m$  is weight of the powder in gram,  $\rho_{\text{tap}}$  and  $\rho_{\text{true}}$  are tap and theoretical densities of powder in  $\text{g}/\text{cm}^3$  respectively. The shearing action of the mixer during the compounding and injection pressure during molding could eliminate major portion of the voids. The residual voids after molding can be calculated by measuring green density of the part and compares it with theoretical green density.

### 3.2 Type of Powders

Two types of stainless steel 17-4PH alloy powder are selected for this study, gas atomized powder 17-4PH-UFP and water atomized 17-4PH Atmix powder (refer to Appendix A for detail on powder atomization processes). The gas atomized powder satisfies well the required qualification for MIM application. Both powders have the same chemical composition containing 16-17% chromium. Table 3.2 shows typical chemistry for these powders.

**Table 3.2** Typical Chemical composition of 17-4PH powder

Alloy Elements	Weight Percentage
Iron (Fe)	Balance
Chromium (Cr)	16-17
Copper (Cu)	3-5
Nickel (Ni)	3-5
Niobium + Tantalum (Nb+Ta)	0.15-0.40
Manganese (Mn)	0-2
Silicon (Si)	0-1
Oxygen (O)	0-0.40
Nitrogen (N)	0-0.03
Carbon (C)	0-0.07
Sulfur (S)	0-0.03

Figure 2a and 2b show the SEM micrograph of the powders. The major difference between these two powders is the particle shape. The gas-atomized powder 17-4PH consists of round powder particle with an average particle size ranging from 8 to 13 microns. The water atomized powder 17-4PH Atmix has semi-round and irregular particle shape ranging from 1 to >23 microns. The theoretical density of the material is 7.78 g/cm<sup>3</sup>.

The tap density of both powders was evaluated by using ASTM B 527-92 procedures. To obtain the tap density, 50 g of powder was weighed in a 50 ml graduated cylinder using an electronic balance with  $\pm 0.1$  gram accuracy. The cylinder is then placed on the tap platform and the locking collar is attached to the platform over the base

of the cylinder. The counter preset to 3000 taps. The machined turned on and allowed to complete the cycle. The volume of the material was recorded by visually gauging the tap level of the material with the corresponding measurement mark on the cylinder. The procedure was used to determine the average tap density of the 17-4PH gas and water atomized powder to be 4.50 and 4.30 g/cm<sup>3</sup> respectively. The 17-4PH gas atomized powder with round particle shape lower value of  $D_{90}/D_{10}$  gained higher tap density. Powders with wide range of particle size will gain higher tap densities. As it is shown in the previous section the particle size distribution could be engineered by mixing two or more different size powders to optimize the tap density.

### **3.3 Stability of Metal Powder in Aqueous Media**

The stability of the powder in aqueous media (aqueous binder system) is the first important factor to consider for powder selection. The stability of 17-4PH gas and water atomized powder evaluated by monitoring the pH of a mixture of metal powder and DI water vs. time at room temperature. The samples were prepared by mixing 15 g of metal powder with 20 g of DI/H<sub>2</sub>O. The pH of the mixture measured initially and periodically for about 60 days. Figure 3.3 presents a comparison result of the several metal powders. The results show that both powders have similar behavior and stability for more than 50 days. Similar results for other powders are shown for comparison. In contrast to the stainless steel powders, the instability of Fe<sub>2</sub>Ni powder can be detected easily. The pH of this powder initially changes rapidly and continues to change with time. This is because the pure iron powder lacks the passivation occurring in stainless steels due to high chromium content. This pure iron powder is not suitable to be incorporated with the

aqueous agar binder system to produce feedstock. The powder quickly oxidizes in contact with the binder and produce iron oxide and hydrogen gas. The instability of this powder could be improved dramatically by adding small amount of sodium silicate or combination of sodium silicate and potassium tetraborate as an additive to the binder formulation [17].

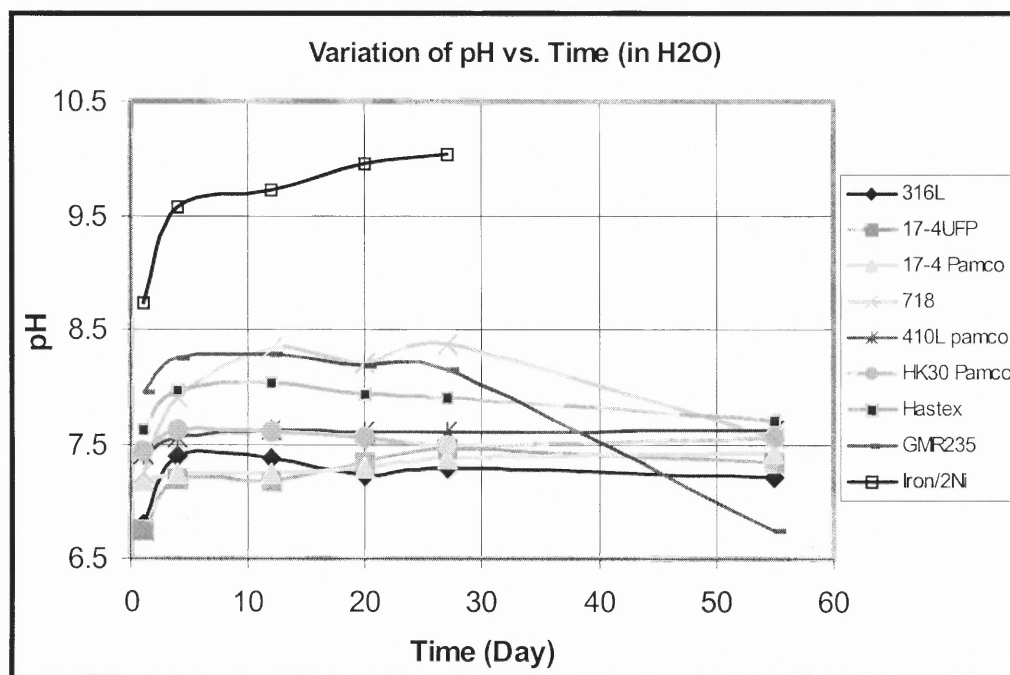


Figure 3.3 Stability of various metal powders in aqueous environment

## **CHAPTER 4**

### **THE AQUEOUS BINDER**

#### **4.1 Agar Binder**

Powdered agar is creamy white, odorless and tasteless. Agar is a hydrophilic colloid extracted from certain marine algae of the class Rhodophyceae [18]. Agar as it is known, is the dried extract from the seaweed of *Gelidium*, *Gracillaria* and other related species of red-purple algae. It is insoluble in cold water, alcohol and most organic solvents, but soluble in boiling water. A 1.5%wt% solution is clear, and when cooled at 32-39°C forms a firm, resilient gel that does not melt below 85°C [19]. Other gums resembling agar but not meeting all the specifications of this definition are termed agaroids.

Agar was discovered by Minoya Tarozaemon [20], a Japanese innkeeper in about 1660. He threw some surplus seaweed jelly into the winter night, expecting it to thaw in the morning sun and disappear into the soil. He found, however, after several days of alternate freezing and thawing, a porous mass that could be re-boiled in water and cooled to yield a gel equal to the original. He had discovered agar.

Agar became popular in Asian regions as food, food ingredient, and medicine. Popularity spread steadily and rapidly, and in about 1866, European use of agar for food began [21]. It is used widely in microbiology, medicine [22], pharmaceuticals and food products for its emulsifying, stabilizing and its gelling properties. In 1881, Dr. Walther Hesse used agar for growing colonies of bacteria [19]. Poller [21] discovered in 1924 that agar gels had the requisite qualities for a moulage material capable of reproducing fine details with great accuracy, thus opening the way for its use as an impression material for criminologists, museum curators, plastic surgeons, and artists. From 1935

onward, dental prosthetics made wide use of agar compositions in precise inlay, crown, and bridge work, as well as in ordinary denture models [23]. Agar is among the most potent gel-forming agents known, for gelation is perceptible at concentrations as low as 0.04% [19]. Low concentration gel is valuable for its protective action, diffusion prevention, and texture enhancement effects. The gelling property and non-toxicity of agar are among the prime reasons for its variety of applications. For the same reason, an agar based binder system was adopted by AlliedSignal / Honeywell [24] to be used for Metal Injection Molding (MIM) and Ceramic Injection Molding (CIM) processes. This binder system will be used as a baseline for this study.

The production of agar starts with collection and washing of seaweed. It is then boiled for 30 to 40 hours, and allowed to settle. The solution is poured into trays and allowed to cool and set. The resulting gel is forced through press holes emerging as stripe, which, are laid out to sun dry. The strips are flaked or powdered and sized. Agar has been known to commerce since 1870 and mainly produced in Chile, Japan, Spain and Morocco. Commercial methods of processing agar include [19]: (1) cleaning raw material, (2) Chemical pretreatment, (3) pressure extraction, (4) chemical post-treatment, (5) filtration, (6) gelation, (7) freezing, (8) post-treatment, (9) washing, (10) drying, (11) sterilization, (12) bleaching, (13) washing, (14) drying. Agar can be efficiently extracted from seaweed with hydrochloric acid solutions of 0.007 M with a 1-hr cooking time [25]. An official specification shown in Table 4.1 [18] has been established to control the level of impurity in agar.

**Table 4.1** Official specification of agar

	Maximum	Minimum
Gelation temperature, 1.5%	39°	32°
Gel melting temperature, 1.5%	—	85°
Moisture	20%	—
Ash	6.5%	—
Ash, acid-insoluble	0.5%	—
Foreign organic matter	1.0%	—
Foreign insoluble matter	1.0%	—
Foreign starch	0	—
Gelatin	0	—
Water absorption	—	5 times its weight
Arsenic	3 ppm	—
Lead	10 ppm	—
Other heavy metals	40 ppm	—

#### 4.2 Viscosity of Agar Gel

In addition to the characteristics of metal or ceramic powder, the viscosity of agar at melting temperature plays an important role on metal and ceramic feedstock solid loading. It will influence the solid content of the feedstock and its flowability during the molding process. The viscosity of the agar gel is affected by its solvent content, temperature and the type of raw material and processing conditions [19]. An agar gel with high solvent content (H<sub>2</sub>O) exhibits lower viscosity at melting temperature. It is desirable to minimize the amount of solvent in the gel and maintain the low viscosity. This will facilitate to reduce the total binder amount and increase the solid loading of the feedstock. Maintaining low viscosity of agar gel binder with low solvent has been investigated by modifying the pH [26] of the solvent (H<sub>2</sub>O), or changing the agar gel composition with an addition of glucose (C<sub>6</sub>H<sub>12</sub>O<sub>6</sub>), sucrose (C<sub>12</sub>H<sub>22</sub>O<sub>11</sub>) and, fructose [27].

The viscosity of agar gel decreases as temperature increases. Figure 4.1 illustrates the apparent viscosity of a 2wt% aqueous solution of agar 100 (from Meer Inc.) at various temperatures [24]. The viscosity of the agar gel at this temperature range reaches its low viscosity at 70°C. The viscosity increases slowly to about 40°C and gelation starts rapidly at about 39°C.

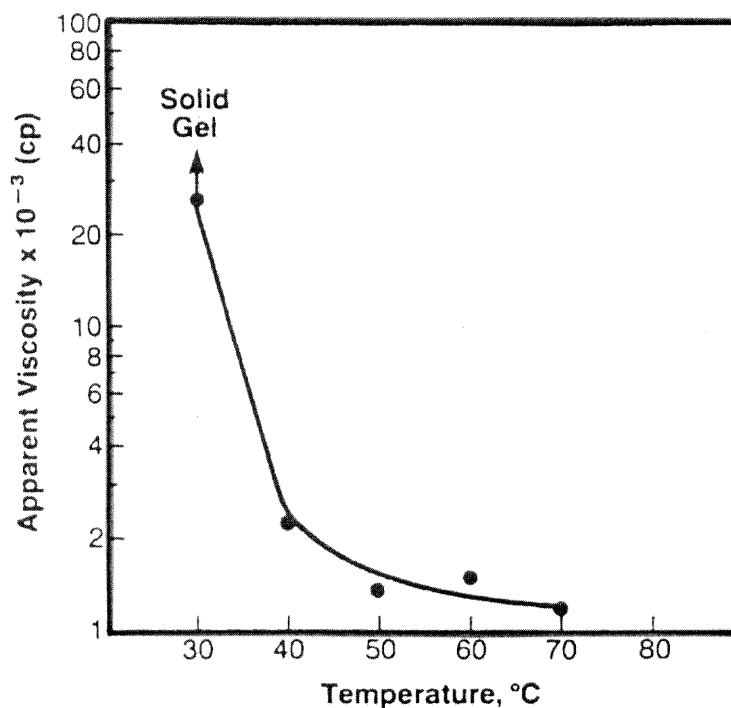


**Figure 4.1** Effect of temperature on viscosity of agar (agar 100 from Meer Inc.) gel.

### 4.3 Study of Gel Strength of Agar Binder

The ability of agar to form strong gels at transition temperature plays an important role on rheology of the feedstock. The effect of agar (TIC100 from TIC Gums, Inc.) concentration on gel strength was studied. The gel strength of agar increases with

concentration of the agar. The gel strength is almost directly proportional to the concentration of agar. The gel strength of six samples having 0.5, 1.0, 1.5, 2.0, 2.5 and 3wt% agar was evaluated. The following is the details of the gel sample preparation and gel strength testing.

#### **4.4. Experimental Procedure**

Sample preparation:

Six gel samples having 0.5, 1.0, 1.5, 2.0, 2.5 and 3wt% agar (TIC100) concentration in DI/H<sub>2</sub>O were prepared. Dry agar was weighed and placed in a clean 250 ml beaker. DI/H<sub>2</sub>O was added to the beaker to bring the total weight to 100 g. A magnetic stirrer bar was placed inside the beaker. Plastic wrap (like Saran Wrap®) was affixed by a rubber band to the beaker with a slight opening at the beaker tip. The beaker was then set inside a 1000w Panasonic microwave oven and heated for approx. three minutes on medium power or until the mixture started to boil. The beaker was placed on the magnetic stirring device for approx. one minute at half speed. The beaker was then placed back into the microwave and the process was repeated twice more. The temperature and the weight of the beaker contents were monitored. The mixture must reach 93-98°C and any weight loss due to evaporation of water was restored. After the heating cycle was completed, the gel was placed in a tray with 2 inches of water at room temperature (24-25°C) for at least one hour. A puncture test apparatus was used to evaluate the gel strength of the samples. Figure 4.2 shows the puncture test apparatus.

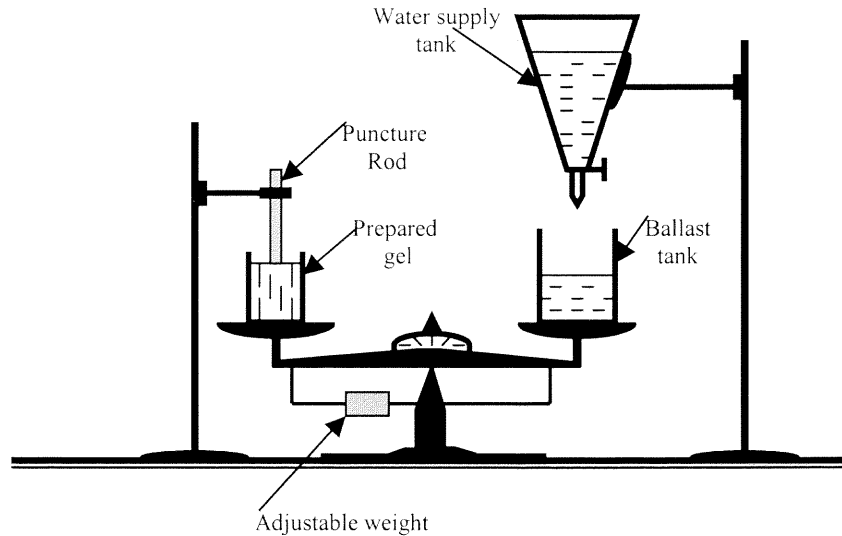


**Figure 4.2** Puncture Apparatus

After the cooling phase, the gel sample is placed on one end of a balance with an empty beaker on the other. The balance was leveled by moving the attached weight on the side of the balance. A one-centimeter diameter aluminum rod was attached to a frame with clamps. The end of the rod was placed so that it comes in contact with the gel surface, but exerts no force. An overhead tank is then allowed to drain into the water ballast tank on the other end of the balance at the rate of approx. 200 g/min. until the rod cleanly breaks through the gel surface.

The amount of water added to the beaker was weighed and recorded for each time. The test was repeated three times to calculate the average gel strength. The gel strength was calculated by dividing the weight of the ballast water at the break point to the rod head surface area.

$$\sigma_{\text{gel}} = W_{\text{H}_2\text{O}} / A_{\text{rod}} \quad (4.1)$$

$$A_{\text{rod}} = \pi r^2 \quad (4.2)$$

$$\sigma_{\text{gel}} = W_{\text{H}_2\text{O}} / \pi r^2 \quad (4.3)$$

$\sigma_{\text{gel}}$  is the gel strength  $\text{g/cm}^2$ ,  $W_{\text{H}_2\text{O}}$  is weight of the water in grams,  $A_{\text{rod}}$  is the rod head surface area in  $\text{cm}^2$ .

Figure 4.3 presents the result of the experiments. It is show that there is a linear relationship between gel strength and Agar content.

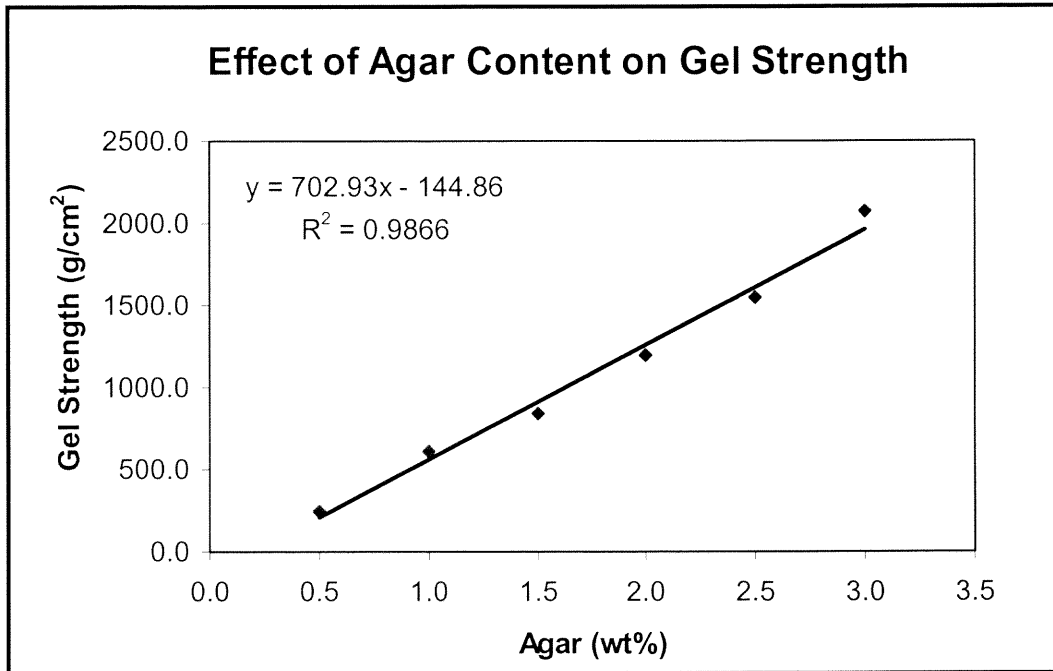


**Figure 4.3** Effect of agar (TIC100) concentration on gel strength

Table 4.2 shows a summary of the experimental result. The gel strength of agar (TIC100) is increases significantly from  $240 \pm 7 \text{ g/cm}^2$  to  $2073 \pm 89 \text{ g/cm}^2$  as the agar concentration increases from 0.5wt% to 3wt%.

**Table 4.2** Effects of agar (TIC100) concentration on gel strength

Agar Concentrations	0.5wt%	1.0wt%	1.5wt%	2.0wt%	2.5wt%	3.0wt%
Gel Strength (g/cm <sup>2</sup> )	240 ±7	615 ±41	846 ±33	1192 ±12	1546 ±51	2073 ±89

## CHAPTER 5

### BINDER ADDITIVES

#### 5.1 Effect of Additives on Gel Puncture Strength of Agar

The effect of gel strengthening additives on gel strength was tested on two types of agar, Meer100 and TIC100. It has been found that the gel strength of these agars is increased when small quantities of additives such as magnesium borate, zinc borate, and calcium borate were added [28]. In this case, the gel strength for fixed amount of agar significantly improved depending on type and the concentration of the additives. This effect plays an important role in feedstock formulation since gel strength enhancing additive substantially reduces the amount of binder needed to provide adequate gel strength. It provides easier part removal from the die cavity, part durability and damage resistively during molding process. Using high gel strength binder could reduce the molding cycle time, which increases the production rate. High gel strength and less binder facilitate shape stability for the molded articles and enhancing dimensional control during sintering. The effect of several borate compounds on gel strength of 2wt% Agar gels was studied. Agar gel samples containing borates of zinc, magnesium, calcium, ammonium, and tetramethylammonium as well as boric acid were prepared and tested following same procedure described previously. Table 5.1 shows the effect of borate compounds on gel strength of both agars gel. The result shows that the gel puncture strength of TIC agar with no additives is substantially better than Meer agar. The data suggests that calcium borate is a preferred gel strengthening additives for both types agar. Other gel enhancing additives shows lesser or insignificant effects.

**Table 5.1** Effect of borate compounds on puncture strength of agar gels

Type of Borate Compound	Gel Strength (g/cm <sup>2</sup> ) (Meer Agar)	Gel Strength (g/cm <sup>2</sup> ) (TIC Agar)
None (control)	817 ±07	1192 ±12
Calcium (0.3 wt%)	1412 ±51	1585 ±60
Calcium (0.45 wt%)	1522 ±51	-
Magnesium (0.3 wt%)	1164 ±37	-
Magnesium (0.45 wt%)	1265 ±41	-
Zinc (0.3 wt%)	1090 ±12	1119±22
Ammonium (0.3 wt%)	948 ±54	-
Ammonium (0.5 wt%)	929 ±60	-
Tetramethylammonium (0.3wt%)	846 ±34	-
Boric Acid (0.3 wt%)	832 ±60	-

## 5.2 New Gel-Strengthening Additive

The effect of a new gel-strengthening additive on gel properties of agar has been studied. The study conducted with two different levels of agar 1.5 and 2wt% containing none, 0.1, 0.2 and 0.3wt% potassium tetraborate tetrahydrate ( $K_2B_4O_7 \cdot 4H_2O$  from Aldrich). The potassium tetraborate unlike the other borate shown in Table 7 is highly soluble in  $H_2O$  at room temperature and does not have tendency to precipitate out of the solution with

time. The stability of 0.4wt% potassium tetraborate concentration in H<sub>2</sub>O was monitored for more than six months. It did not show any sign of precipitation.

Aqueous solution containing of 0.1, 0.2 and 0.3wt% potassium tetraborate was prepared. The first set of gel samples was prepared by adding 1.5wt% agar to potassium tetraborate solutions. Same gel preparation and gel strength measurement procedure, which, previously described was followed. The average strength of gel containing 1.5wt% agar at three concentration levels of potassium tetraborate is shown in Figure 5.1.

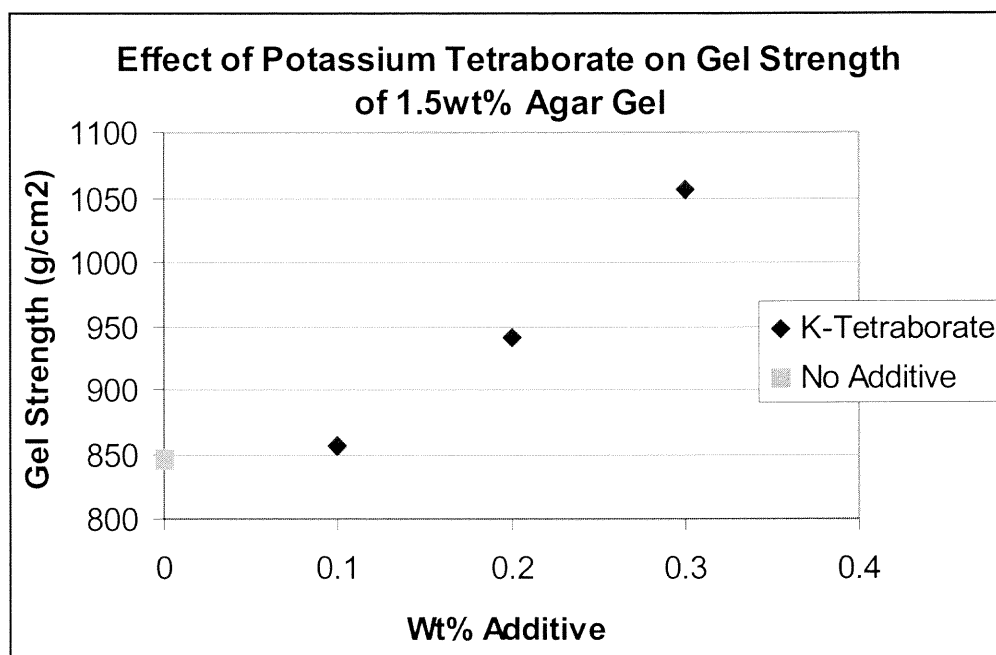


**Figure 5.1** Effect of potassium tetraborate on gel strength of 1.5wt% agar gel

The gel strength of the agar proportionally increased as the concentration of the potassium tetraborate increased from 0.1 to .03wt%. At low concentration of 0.1wt% borate the effect was not significantly changed from virgin agar. Table 5.2 Illustrates a summary of the result.

**Table 5.2** Effect of potassium tetraborate on gel strength of 1.5wt% agar concentration

Potassium tetraborate Concentration (wt%)	None	0.1	0.2	0.3
Gel Strength (g/cm <sup>2</sup> )	846 ±33	856 ±14	941 ±20	1055 ±17

The second set of gel samples was prepared with same levels of potassium tetraborate concentrations of 0.1, 0.2, 0.3wt% using 2wt% agar. The average gel strength of these samples was evaluated. The gel strength of 2wt% agar containing 0.3wt% of calcium, zinc, and lithium metaborate and lithium tetraborate was also tested and compared with potassium tetraborate additive. Figure 5.2 presents the effects of potassium tetraborate additive on gel strength of 2wt% agar (TIC100) gel. The summary of the results in Table 5.3 indicates that the gel strengthening effect of potassium tetraborate is more effective than the other types of borate at an equal concentration.

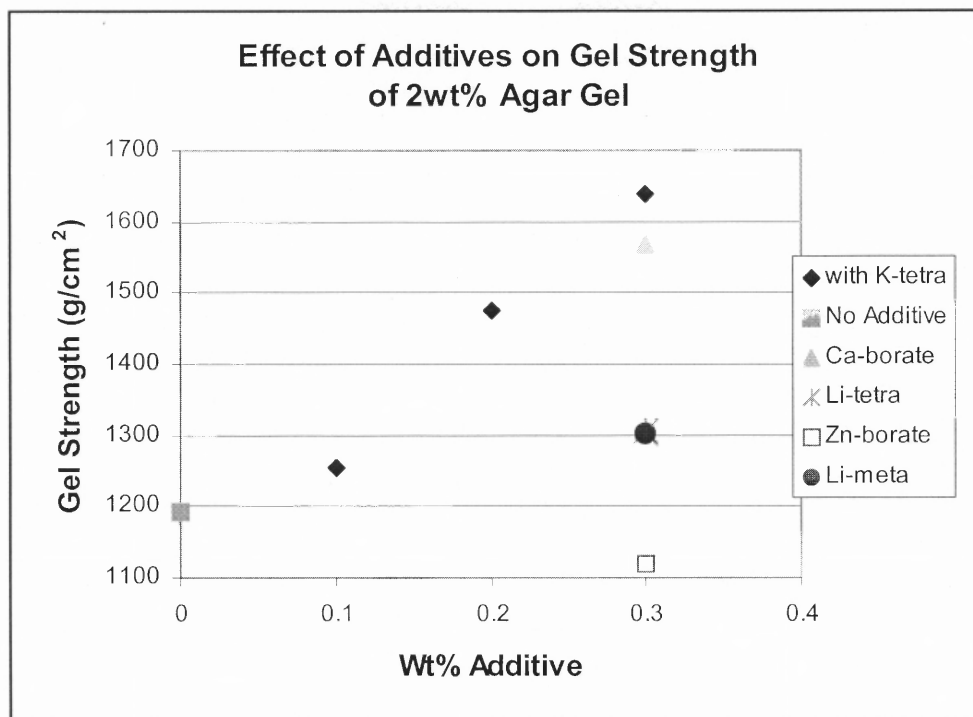


**Figure 5.2** Effect of potassium tetraborate on gel strength of 2wt% agar gel

**Table 5.3** Comparison effect of different additives on gel strength of 2wt% agar gel

Concentration of Gel Strengthening Additive (wt%)	Gel Strength (g/cm <sup>2</sup> )
Agar (No Additive)	1192 ±12
Potassium Tetraborate (0.1wt%)	1256 ±28
Potassium Tetraborate (0.2wt%)	1476 ±17
Potassium Tetraborate (0.3wt%)	1639 ±16
Calcium Borate (0.3wt%)	1569 ±46
Zinc Borate (0.3wt%)	1306 ±45
Lithium Tetraborate (0.3wt%)	1303 ±55
Lithium Metaborate (0.3wt%)	1119 ±22

Among the other advantages of using potassium borate as a gel strengthening additive are good solubility and cost effectiveness of this additive. Calcium borate is partially soluble in water. This will limit the desired concentration of this additive in the H<sub>2</sub>O. Because of this limitation, the addition of this additive was performed by reaction of calcium oxide and boric acid in pH controlled H<sub>2</sub>O. The process is time consuming and expensive. One liter of in-situ H<sub>2</sub>O containing 0.2wt% calcium borate costs about \$43 with this process. In addition to cost the calcium borate is not stable and precipitate out of the solution with time. In comparison, the potassium borate is highly soluble in H<sub>2</sub>O and it is very stable in the solution. The cost is significantly lower \$0.03-0.04/gram of dry powder. Consequently, the cost of one liter of in-situ water with this additive was extensively lower about \$0.06. The preparation of in-situ water with this additive was simply accomplished by mixing and stirring for 5 minutes.

## CHAPTER 6

### THE AQUEOUS BASELINE METAL FEEDSTOCK

#### 6.1 Baseline Formulation

The baseline feedstock composition comprises of 17-4PH gas or water-atomized metal powder, agar gel as a main binder constituent. The agar gel contains about, 7.5-8wt% water, as a gel forming liquid. A mixture of two types of biocides, Methyl-p-Hydroxybenzoate ( $C_8H_8O_3$ ) and Propyl-p-Hydroxybenzoate ( $C_{10}H_{12}O_3$ )(from Penta Manufacturing) was incorporated with the agar gel. The total biocide is about 1.6wt% based on the agar amount in the formulation. The function of the biocides is to prevent the growth of bacteria and degradation of the agar gel binder in the feedstock. The baseline feedstock composition contains 89.9wt% (55.1vol%) 17-4PH powders, 2.1wt% (6.7vol%) agar (TIC100) containing biocides and 8wt% (38.2vol%) D.I/H<sub>2</sub>O. This baseline composition has been used with water or gas atomized 17-4PH stainless steel powder to make experimental and production feedstock batches.

The baseline formulation for metal is applicable for compounding ceramic feedstock. The amount of binder content for ceramic feedstock formulation varies from 2-4wt% depending on the type of ceramic powder being used. For most of the ceramics powders such as aluminum oxide, silicon nitride and bone china, compounding the feedstock material starts with slip preparation and optimization. The prepared slip must be stable and not change its viscosity with time prior to mixing with agar binder. For example, MIM aluminum oxide feedstock was made from aluminum oxide powder (C90 alumina powder from Alcan Co.) [42]. The powder was mixed with de-ionized water, which contained 0.2-1wt% ammonium polyacrylate solutions as dispersant additives.

The pH of the water adjusted to 9-10 using tetramethyl ammonium hydroxide. The mixture was milled for about 24 hours with alumina milling media. The resulting slip was transferred to a sigma blender and mixed with 2-3wt% agar at 85-95°C for one hour. The compounded feedstock was cooled to room temperature and shredded. The feedstock material showed good moldability at 17-17.5% moisture content. In another example, recycled bone china ceramic powder was incorporated with the agar binder system to formulate bone china feedstock for injection molding process [43]. The preparation steps of this feedstock are similar to aluminum oxide feedstock. Refer to the patents for complete details on feedstock formulations, and processing steps of these ceramics feedstock materials (reference 42 and 43).

## **6.2 Experimental Batch Using Water Atomized Powder**

Several experimental batches were made using 17-4PH (Atmix) water atomized powder. Each batch was made with 6400 grams of metal powder, 134.4 grams agar (TIC100) containing biocides and 700 grams of D.I/H<sub>2</sub>O. The agar powder was mixed with the D.I water at room temperature and then transferred into a sigma mixer. The mixture gradually heated to 95°C (205°F) with continuous mixing until the agar mixture was completely melts. Half of the metal powder was added to the melted agar and mix for 15-20 minutes. The rest of the powder was added and mixed for 45-60 more minutes. The compounded batch was allowed to cool to 38°C (100°F) and then removed from the mixer. Removing and shredding the compounded batch becomes very difficult at lower temperature due to the rigidity of the material. The compounded batch was shredded to small particulate, using a Hobart (Model PF350) shredder shown in Figure 6.1a.

The moisture content of the feedstock was evaluated using a Computrac<sup>®</sup> MAX-2000XL Arizona Moisture Analyzer shown in Figure 6.1b. It accurately detects moisture levels from 50 PPM to 100% and accommodates sample weights of 150 mg to 40 grams. The heating range is 25°C to 275°C, controlled to an accuracy of  $\pm 1^\circ\text{C}$ .

A feedstock sample about 36 grams was placed into the analyzer compartment. Analyzer automatically records the initial weight of the sample, and then gradually raised its temperature to 160°C (320°F), and holds the temperature until the sample was completely dried (about 10-15 minutes). The analyzer uses the initial (undried) and the final (dried) weight to calculate the moisture content of the feedstock using following expression.

$$\% \text{Moisture} = [(W_u - W_D)/W_u] 100 \quad (6.1)$$

Where  $W_u$  is undried and  $W_D$  is dried weight.

The moisture content of the feedstock sample was measured to be 8.36wt% (91.64wt% solid). The batch was initially formulated with 9.86wt% (90.14wt% solid) moisture content to compensate for any moisture lost during the batch mixing and preparation.

The difference between the starting and final moisture content shows that 1.5wt% moisture was lost during the batch preparation. The moisture content of this batch was adjusted to 8wt% (92wt% solid). The excess moisture of 0.36wt% was removed by evaporation. A rotary drier was used to remove the excess moisture from the feedstock.

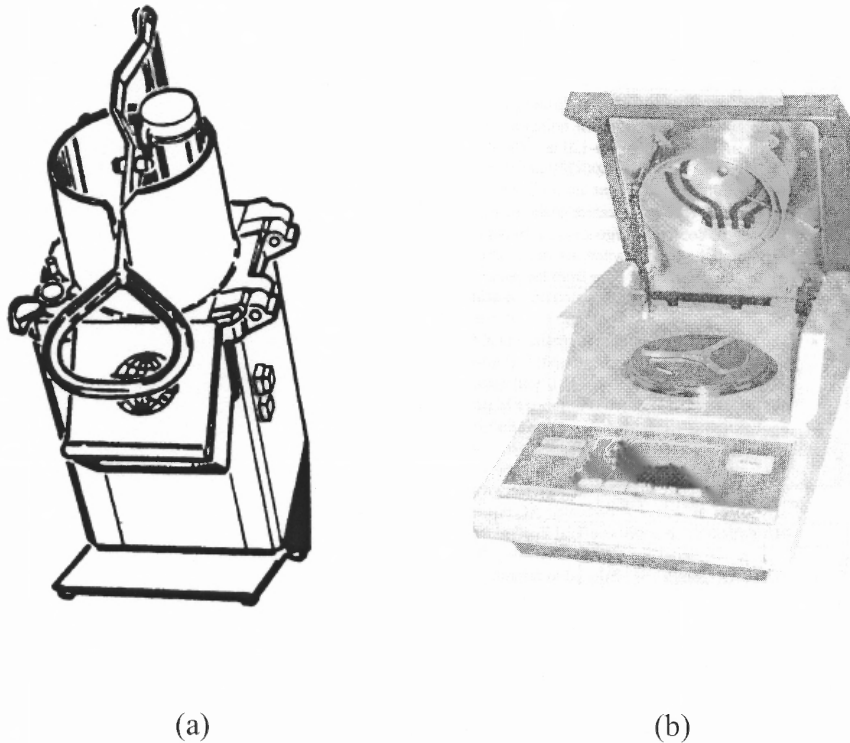


**Figure 6.1** Schematic of (a) Hobart Shredder, (b) Arizona Moisture Analyzer

The target moisture was achieved by determining the initial moisture content of the material using Arizona moisture analyzer and weight lost calculation by applying the following expression.

$$W_t = W_i (1 - M_i/100)/(1 - M_t/100) \quad (6.2)$$

Where  $W_t$  is target weight,  $W_i$  initial weight,  $M_i$  initial moisture, and  $M_t$  the target moisture. The target moisture is selected and insert in the equation. Since target moisture, initial weight and, initial moisture are known, the target weight is calculated.

The target weight, which represents the target moisture, is reached by evaporating or adding moisture to the feedstock material. Other batches were compounded with 17-4PH water atomized (Atmix) powder at 8.5 (91.5wt% solid), 7.5 (92.5wt% solid) and 7wt% (93wt% solid) moisture levels to study the effect of moisture content on flowability.

### **6.3 Flow Characteristics of Baseline Formulation**

Apparatus:

Injection Molding Machine:

A hydraulic Boy 22M injection molding machine from Boy Machines Inc. was used to study the flow characteristics of various feedstock compositions. The barrel capacity of the machine is about 0.9 oz and has a 1:1 compression screw. The barrel has four zones, heated with four separate electric heating bands with maximum temperature of 450°C (841°F). The machine operating and molding variables can be adjusted through a control panel. The machine has three operating modes: manual, semi-automatic and automatic. The clamp pressure range is 51-163.1 kg/cm<sup>2</sup> (725-2320psi). The maximum injection and holding pressure capability is 163.1kg/cm<sup>2</sup> (2320psi). The screw rotation speed ranges from 0-250 rpm. The injection speed capability of the machine is 0-160 mm/sec. The back pressure ranges from 0-51 kg/cm<sup>2</sup> (0-725psi).

### **6.4 Spiral Flow Mold**

Figure 11 shows "A", "B" sides, and the cavity of spiral mold (MUD Quick Change<sup>T. M.</sup> 84/90 T Style) designed for testing the flow of various thermoplastic materials. The mold is constructed with a 65-inch flow distance and is engraved in one-inch increments to

allow for easy flow comparisons. The cross section is approximately 0.125 inch deep and 0.225 inch wide and is trapezoidal in design. The cavity area is polished to SPE-SPI number 2 finish. The mold has a center gate with 0.2-inch diameter. The mold equipped with a Cincinnati Milacron water heater to control the mold temperature.

Spiral mold was developed to better evaluate the moldability of material [29]. The spiral flow is an excellent method for comparing flow properties of different batches of the same material and of the same material from different source [30]. It is used as a common practice to measure the flow characteristics of various thermoplastic materials. The effects of various additives and their amounts on flow behavior of material can be evaluated by spiral flow testing. It is used to determine the effect of changing various molding conditions such as injection speed, melt temperature of material, and mold temperature on flow properties. The flow data also can assist the part designer in making gate decisions, especially for parts of constant wall thickness [31].

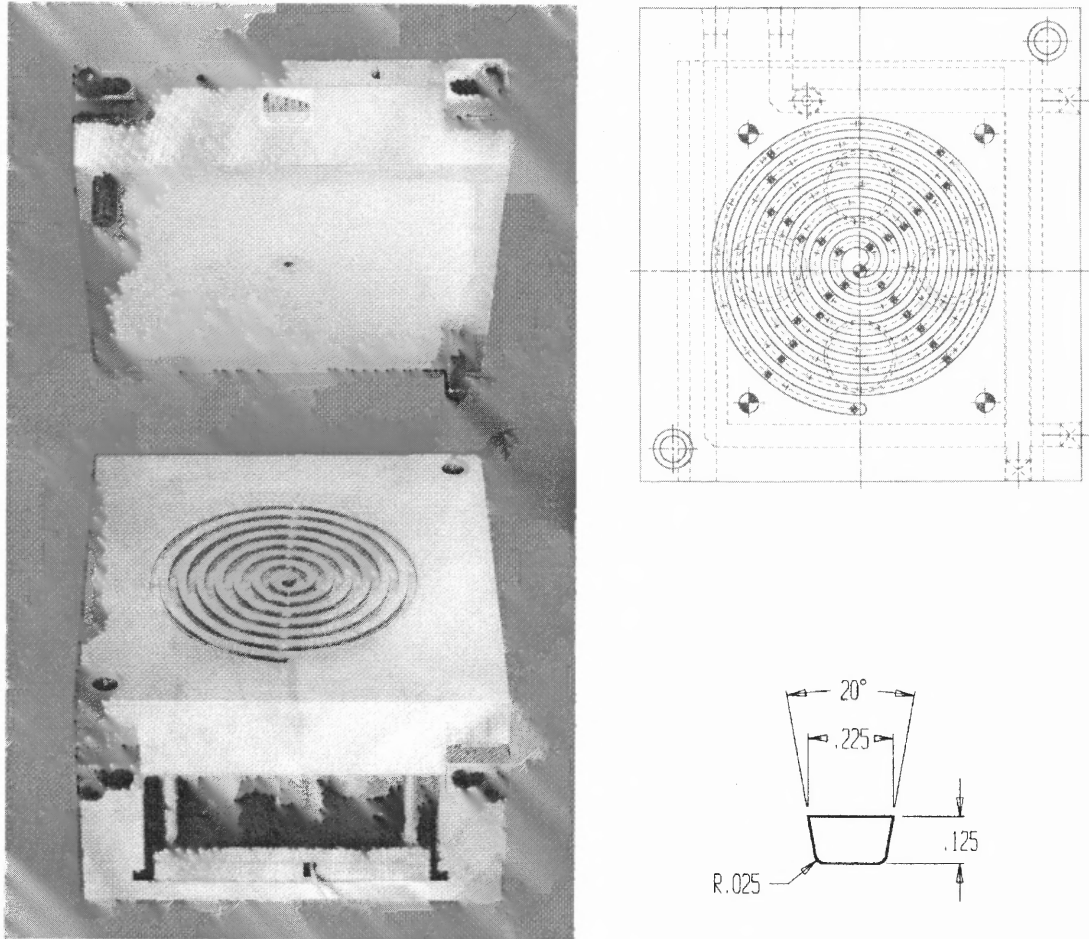


**Figure 6.2** (a)“A” and “B” sides of the spiral mold and, (b) the cavity of spiral mold

The flow characteristics of the 17-4PH (Atmix) water atomized baseline feedstock composition have been investigated. The flow behavior was studied as a function of solid loading at 500, 1000 and 1500 psi injection pressure. The center gated spiral die shown in Figure 6.2 was used to evaluate the flow variation of the feedstock material. The molding conducted under a fixed set of conditions. Table 6.1 presents the applied molding conditions for the flow experiments.

**Table 6.1** Machine setting for spiral flow testing

<b><u>Temperatures:</u></b>	
Barrel Temperature °C (zone: 1,2,3, nozzle)	54.5, 83, 83, 83
Mold Temperature °C	22
<b><u>Speed:</u></b>	
Screw Recovery Speed (rpm)	55
Injection Speed (in/sec.)	25
<b><u>Pressures:</u></b>	
Injection Pressure (psi)	500, 1000, 1500
Holding Pressure (psi)	None
Back pressure (psi)	5
<b><u>Plasticizing:</u></b>	
Plasticizing Delay (sec.)	0.1
Decompression (mm)	Non
Shot Size	50% of Barrel Capacity

## 6.5 Experimental Procedure

The moisture content of four experimental batches of 17-4PH water atomized (Atmix) feedstock was adjusted to various levels ranging from 8.97 to 7.1wt%. The molding parameter listed on Table 4.3 was dialed into the Boy 22M injection molding machine and the barrel temperature of the machine was allowed to reach its set point temperature

of 83°C (180°F). The mold temperature was set at 22°C. The hopper of the machine was filled up with the shredded feedstock and the screw was manually rotated to transfer the feedstock into the hot zone of the barrel. The machine was set on semi-automatic mode. The mold was closed and molten feedstock was injected into the spiral mold cavity at 63 cm/sec. (25 in/sec). The molded spiral sample cooled in the mold for 10 second. After the cooling time expired, the mold was opened and spiral sample ejected from the mold. The samples were collected and dried at room temperature for 30-45minutes and, flow distance of each sample was recorded. The flow characteristics of the feedstock were tested at 500, 1000 and 1500psi injection pressures. Ten spiral samples were molded at each injection pressure level. The average flow of the feedstock calculated and recorded to compare with the feedstock material having different moisture content.

Four batches of 17-4PH (Atmix) baseline composition were compounded at different moisture levels for flow evaluation. The moisture content of these batches was adjusted to 8.97wt% (91.03wt% solid), 7.93wt% (92.07wt%), 7.40wt% (92.60wt%) and, 7.1wt% (92.9wt%). Spiral flow analyses of these batches was conducted at 500, 1000, and 1500psi injection pressure.

## 6.6 Results

The effect of injection pressure on flowability of the 17-4PH (Atmix) baseline feedstock material was evaluated. The flowability of four batches was studied at 91.03, 92.07, 92.60, and 92.90wt% solid content. Figure 6.2 depicts the flow behavior of the feedstock material vs. injection pressure. The flowability of the feedstock material increases as injection pressure increases. The average flow distance of the feedstock material having

91.03wt% solid was increased from 8.6 to 19.5 inches as injection pressure increased from 500 to 1500psi. It is also shown in Figure 6.2 that the flow distances are shifted to lower values at any injection pressure, as the solid content increases. The flow characteristic significantly affects the moldability behavior of the materials. The moldability of the material deteriorated as the flowability of the material decreases.

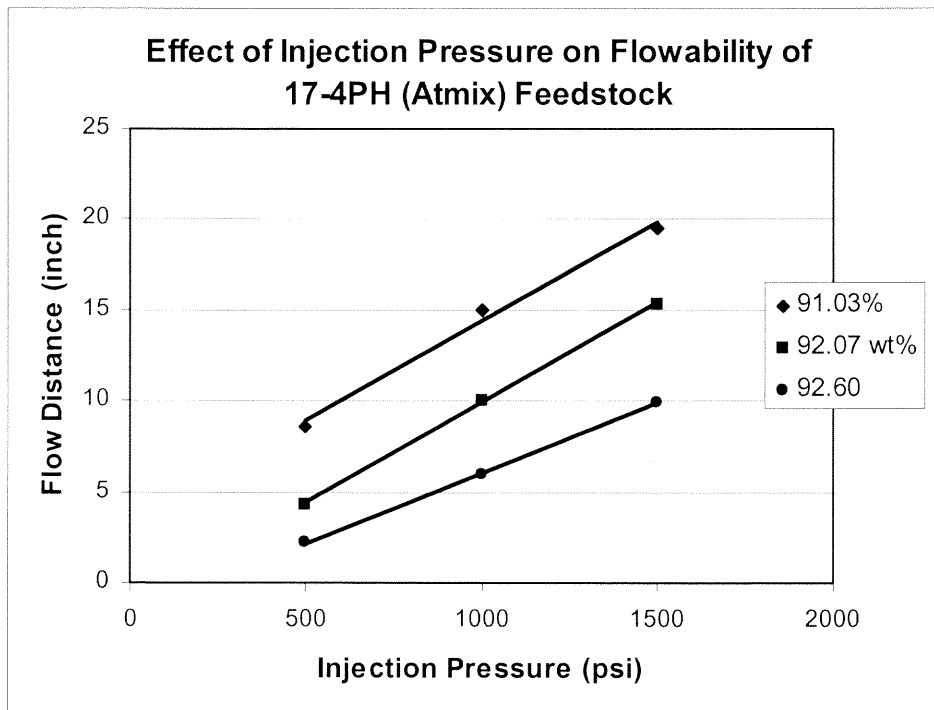


**Figure 6.3** Effect of injection pressure on flowability of 17-4PH (Atmix) baseline compositions

The flowability was also affected by the solid content of the feedstock material. Figure 6.3 illustrate the effect of solid % on flowability of 17-4PH (Atmix) baseline feedstock material at 500 and 1000 psi injection pressure. The flowability decreases as the solid content of the feedstock increases. The flow length decreases from 8.56 to 2.15 inch as the solid content increases from 90.03wt% to 92.60wt% solid at 500 psi injection

pressure. Similar effects have been observed at 1000 psi injection pressure. When the solid content increases from 90.03 to 92.60wt%, the flowability also decreases from 15.0 to 5.9 inches. The flow becomes very sensitive to solid loading higher than 92.6wt%. It reached its critical solid loading at 92.9wt% solid, where the material completely lost its flowability. The flow behavior of the material improves as solid loading moves away from critical solid loading. The optimum solid loading for the 17-4PH (Atmix) baseline composition is determined to be  $0.4 \pm 0.1$ wt% lower than the critical solid loading. The feedstock material at this solid loading demonstrated proper flowability for molding.

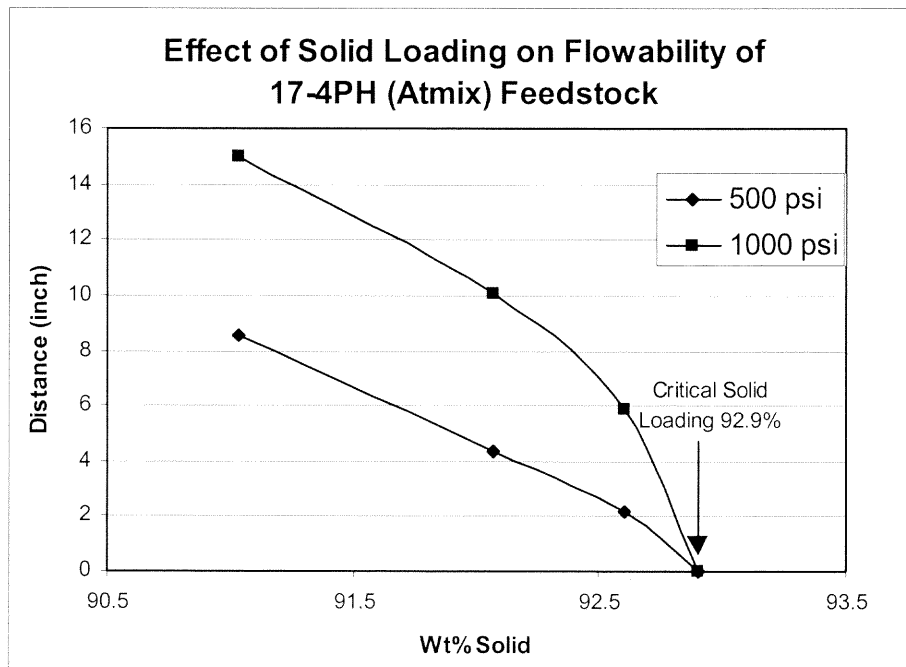


**Figure 6.4** Effect of solid loading on flowability of 17-4PH (Atmix) baseline compositions

### **6.7 Experimental Batch Using Gas Atomized Powder**

Five experimental batches were made using 17-4PH (UFP) gas-atomized powder. The batches were made with 6400 grams of metal powder, 134.4 grams agar (TIC100) containing biocides and 700 grams of D.I/H<sub>2</sub>O. The agar powder was mixed with the D.I water at room temperature and then transferred into a sigma mixer. The mixture was gradually heated to 95°C (205°F) with continuous mixing until the agar mixture completely melts. Half of the metal powder was added to the melted agar and mixed for 15-20 minutes. The rest of the powder was added and mixed for 45-60 more minutes. The compounded batch was allowed to cool to 38°C (100°F) and then removed from the mixer and shredded to small particulate. The moisture content of these batches was adjusted to various levels to study the flow characteristics of the baseline feedstock composition containing gas-atomized powder.

### **6.8 Experimental Procedure**

The moisture content of five experimental batches of 17-4PH gas-atomized (UFP) feedstock was adjusted to 8.97wt% (91.03wt% solid), 7.93wt% (92.07wt%), 7.31wt% (92.69wt%), 6.9wt% (93.1wt%) and, 6.7wt% (93.3wt%) to be used for spiral flow evaluation. The molding parameter listed on Table 10 was dialed into the Boy 22M injection molding machine and the barrel temperature of the machine was allowed to reach its set point temperature of 83°C (180°F). The mold temperature was set at 22°C. The hopper of the machine was filled up with the shredded feedstock and the screw was manually rotated to transfer the feedstock into the hot zone of the barrel. The machine was set on semi-automatic mode. The mold was closed and molten feedstock was

injected into the spiral mold cavity at 63 cm/sec. (25 in/sec). The molded spiral sample cooled in the mold for 10 second. After the cooling time expired, the mold was opened and spiral sample ejected from the mold. The samples were collected and dried at room temperature for 30-45minutes and, flow distance of each sample was recorded. The flow characteristic of the feedstock was tested at 500, 1000 and 1500psi injection pressures. Ten spiral samples were molded at each injection pressure level. The average flow of the feedstock was calculated and recorded to compare with the feedstock material having different moisture content.

Five batches of 17-4PH (UFP) baseline composition were compounded at about 10wt% moisture content. The moisture content of these batches was adjusted to 8.97wt% (91.03wt% solid), 7.93wt% (92.07wt%), 7.30wt% (92.70wt%), 7wt% (93.0wt%) and 6.7wt% (93.3wt%), to investigate the effect of injection pressure and moisture level on flowability of the feedstock. Spiral flow evaluation was conducted on these batches at 500, 1000, and 1500psi injection pressure.

## 6.9 Results

The effect of injection pressure on flow behavior of the baseline feedstock composition containing gas-atomized (UFP) powder was evaluated. The spiral flow experiment was conducted on this material at 500, 1000, and 1500 psi injection pressure. Figure 6.4 shows that the flow length increases as the injection pressure increases from 500 to 1500 psi. The highest flow length demonstrated by the feedstock material containing 8.97wt% moisture content. The flow distance shifted to lower values for the feedstock material with lower moisture content. The result shows a linear relationship between flowability

and the injection pressures. However, the material becomes less responsive to applied pressure at lower moisture content. This can be observed by examining the slope of the lines. The slope value reduces by about 36% as the solid content changes from 91.0 to 93.10wt%. In comparison with 17-4PH (Atmix) feedstock, this material shows better flowability at 500, 1000 and 1500 psi injection pressures.

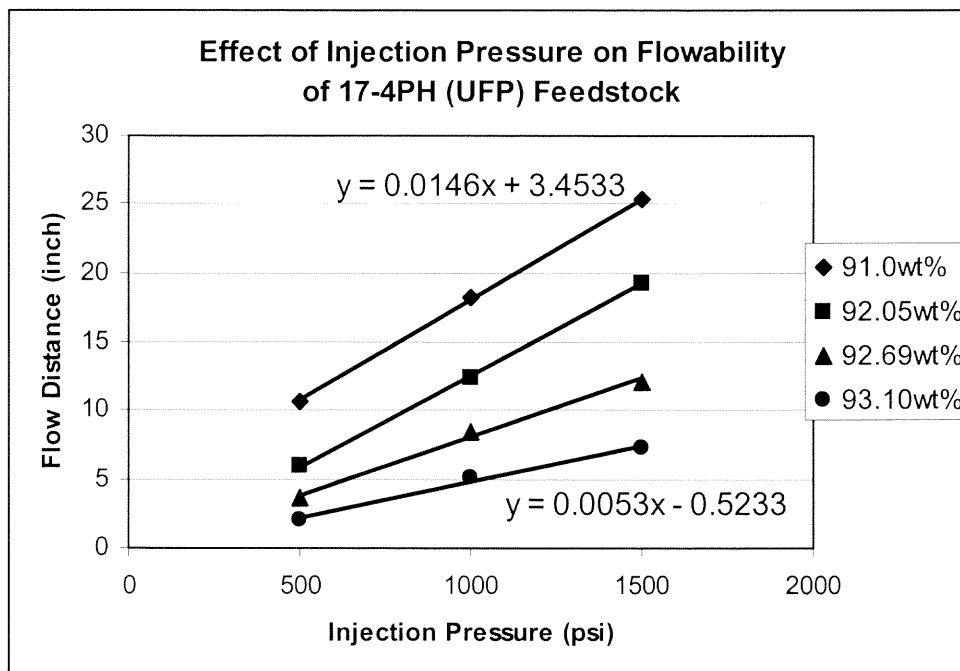


**Figure 6.5** Effect of injection pressure on flowability of 17-4PH (UFP) baseline compositions

The flow characteristic of the baseline feedstock comprising 17-4PH (UFP) gas-atomized powder was effected by solid loading. Figure 6.5 shows that the flow was effected by the solid loading. The flow distance become shorter as the solid content of the feedstock increases. The flow starts decreasing drastically at solid content greater than 92.7wt% and reaches zero value at critical solid loading of 93.3wt%. A feedstock material that shows the ability to flow greater than 2.5 and 6.5 inches at 500 and 1000psi

for a particular solid loading is considered a moldable material at that solid loading. The 17-4PH (UFP) feedstock material indicates sufficient flowability at 92.7 and 92.8wt% solid loading for molding. The result shows that this feedstock material could be molded at 92.7wt% with no difficulty.

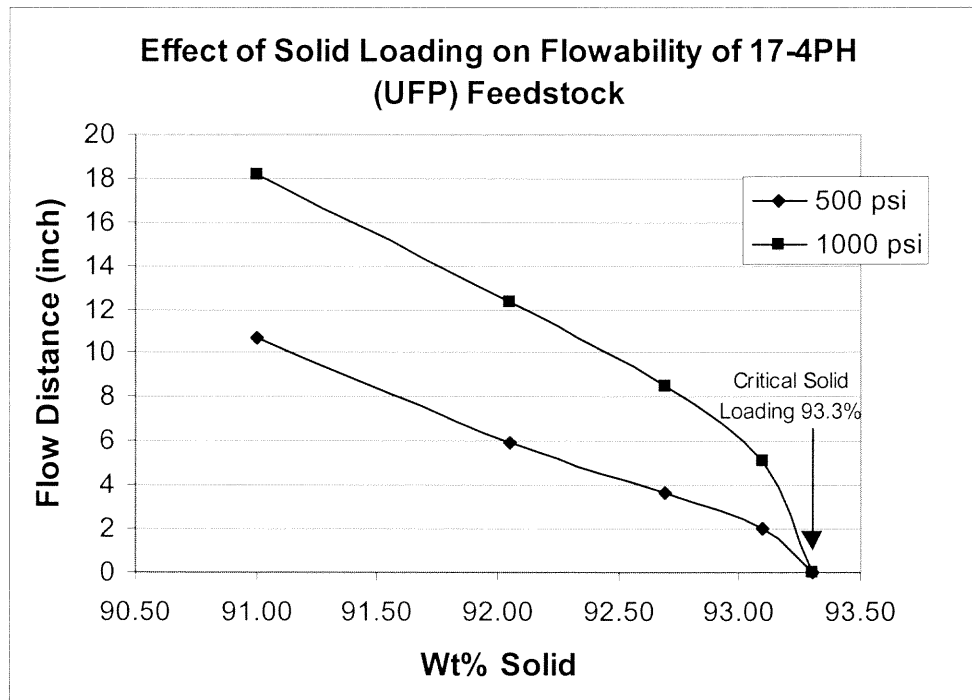


**Figure 6.6** Effect of solid loading on flowability of 17-4PH (UFP) baseline composition

In comparison with 17-4PH (Atmix) water-atomized feedstock, the gas atomized feedstock material demonstrates higher flowability. For example, the 17-4PH gas-atomized feedstock at 92.7wt% solid and 1000psi injection pressure flows about 44% more than water atomized material. The flow differences between gas and water atomized feedstock material is clearly associated to the characteristics of the starting powder, since both feedstock materials were prepared with an identical formulation and mixing procedures.

## CHAPTER 7

### BINDER SYSTEM COMPONENTS

#### 7.1 Effect of Binder System Components on Density of the Feedstock

It is desirable to increase the density of feedstock material to a maximum possible level. Feedstock material with high density pushes the solid loading and weight of the green part to a higher value resulting in lowering the final shrinkage and increasing sintered density, other factors being equal. In a simple polymer binder system, which primarily deals with one type of binder component, higher feedstock density is achieved by reducing the binder content and increasing the metal powder accordingly. The maximum solid loading is based on the critical solid loading of each powder-binder system. The critical solid loading is an experimentally determined parameter that varies with each powder-binder system [32].

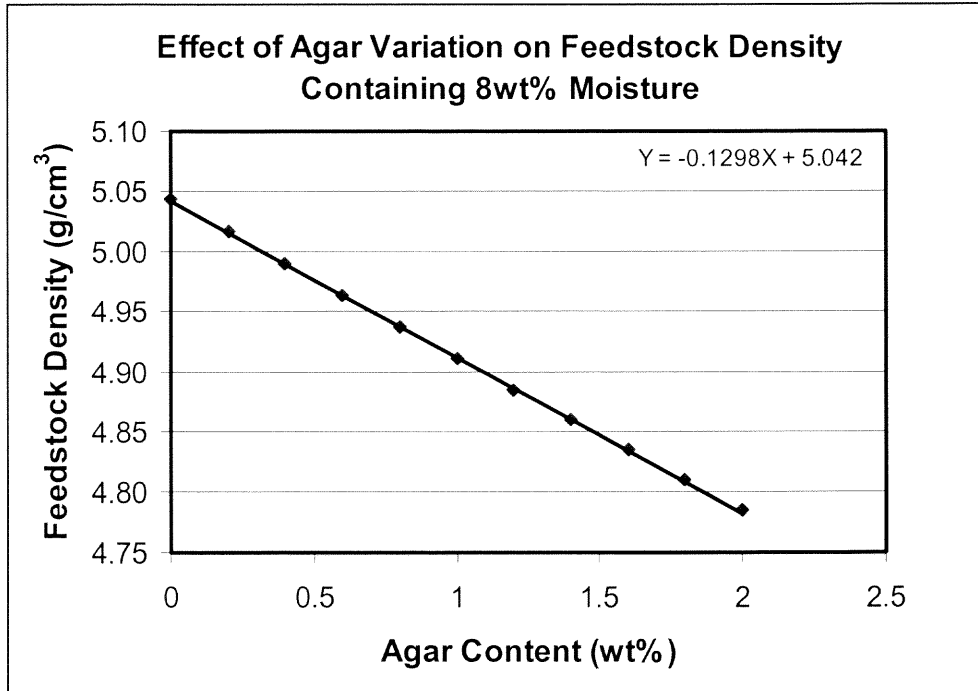
Unlike the polymer binder system, the agar binder system is composed of two major components, i.e.; agar powder and DI water, as well as, minor amount of two types of biocide additives, methyl-p-Hydroxybenzoate and Propyl-p-hydroxybenzoate. Each of these components can have a different effect on the density of the feedstock material. The theoretical density of the feedstock as a function of water and agar was calculated to evaluate the effect of these components on the density. The effect of the biocides was not included in the calculation because the amounts of these additives are not significant in the feedstock formulation. First, the density of 17-4PH feedstock material containing 8wt% moisture was calculated as a function of agar content. The density of the feedstock was calculated using the following expression.

$$\rho_{fs} = W_1 / (W_2/\rho_2 + W_3/\rho_3 + W_4/\rho_4) \quad (7.1)$$

Where  $\rho_{fs}$  is density of the feedstock,  $W_1$ ,  $W_2$ ,  $W_3$ , and  $W_4$  are weight of the feedstock, weight of metal powder, weight of agar and weight of the water in grams respectively.

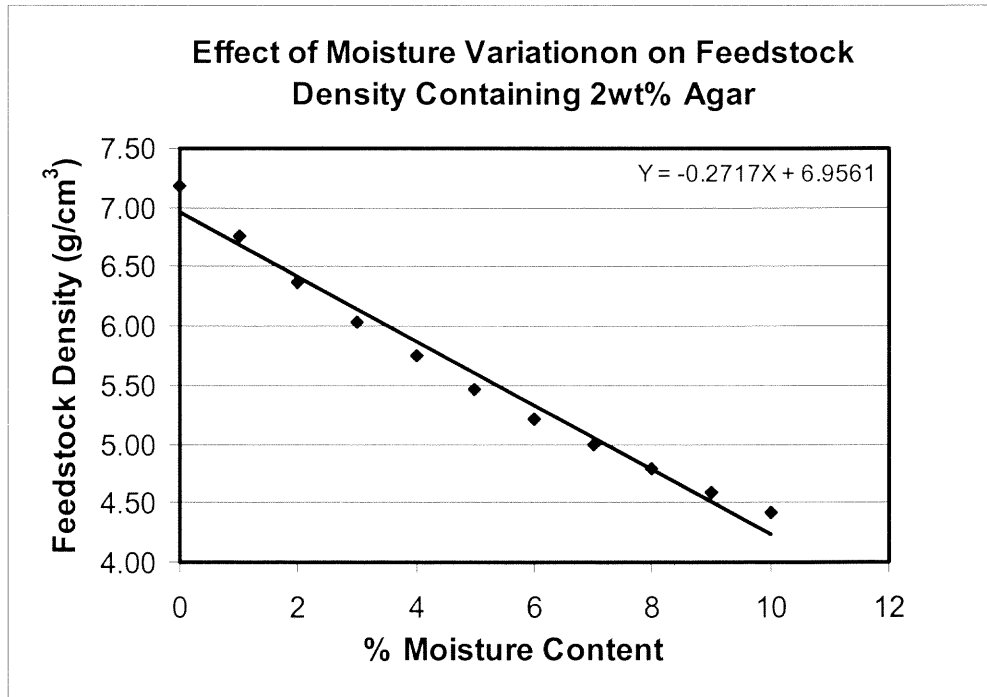
$\rho_2=7.78$ ,  $\rho_3=1.51$  and,  $\rho_4=1$  are the densities of metal powder, agar and water in g/cm<sup>3</sup>.

Figure 7.1 shows the effect of agar variation on density of the feedstock.



**Figure 7.1** Effect of agar content on density of stainless steel 17-4PH feedstock

The effect of water content on theoretical density of 17-4PH feedstock material containing 2wt% agar powder was evaluated. The density of the feedstock calculated as a function of moisture variation in the feedstock formulation using equation (7.1). Figure 7.2 predicts the effect of moisture variation on density of 17-4PH feedstock. The straight line was drawn through the calculated data points for comparing with the slope in Figure 7.1.



**Figure 7.2** Effect of moisture content on feedstock density containing 2wt% agar

The result shows that reducing both water and or agar in the feedstock formulation increases the density of the feedstock. However, reducing the water content increases the density of the feedstock more effectively. Reducing the moisture content by 1% the density increases by 3.90%, whereas the reduction of agar by 1% improves the density by 2.57%. The reduction of moisture improves the density of the feedstock by 51.7% more than reducing the agar content. By the same token, reducing the moisture content more effectively increases the solid loading of the feedstock.

## 7.2 Effect of Additives on Rheology of 17-4PH Feedstock

Improving the solid loading of the feedstock is among one of the key factors that influences the molded green weight, sintered density and final shrinkage of the molded article. It was pointed out in the previous section that reducing the moisture content more effectively increases the solid loading of the feedstock. It also showed that the critical solid loading of the baseline composition 17-4PH (Atmix) water atomized and (UFP) gas atomized feedstock formulation can not be exceeded more than 92.9 and 93.3wt%, respectively. The flowability of the 17-4PH (Atmix) feedstock sharply decreased at solid loading greater than 92.6wt%, thus a loading near 92.50wt% is preferred, for the fixed solid loading (metal + agar) of 90.5wt% and 2wt%. Similarly, the 17-4PH gas atomized feedstock shows rapid increase in viscosity at solid loadings higher than 93.1wt% making flow. The preferred solid loading for this material was 92.7-92.8wt%, for the fixed metal, agar solid loading of 90.8wt% and 2wt%. These solid levels are called the maximum or optimum solid loading of the feedstock. At maximum solid loading, the feedstock materials have lowest possible moisture with proper flowability for molding.

It is desirable to minimize the moisture content (increase the metal solid loading) of the feedstock beyond its maximum solid loading and maintain sufficient flowability. For this purpose, several additives were studied. Three types of additive, i.e. glucose (D-Glucose, Anhydrous  $\text{CH}_2\text{OH}(\text{CHOH})_4\text{CHO}$  from Fisher), sucrose, and fructose were evaluated. Initially, several binder compositions were designed with glucose additives and used for compounding 17-4PH (UFP) gas atomized powder. The first experimental feedstock composition "A" was compounded with glucose additive, containing total of 2wt% binder (agar + glucose) with agar/glucose ratio of 2.2.

### 7.3 Experimental Procedures

A mixture of 50 grams glucose and 680 g of DI/H<sub>2</sub>O was stirred at room temperature until the glucose completely dissolved. Agar powder was pre-mixed with 1.6 and 1.2 grams of methyl-p-hydroxybenzoate and propyl-p-hydroxybenzoate respectively. The water-glucose solution was added to 110grams of TIC agar powder and mixed thoroughly. The mixture was placed in a sigma mixer and gradually heated to 95°C (205°F) with continuous mixing until the binder was completely melted. A total of 7842 grams of 17-4PH (UFP) gas-atomized powder was added to the binder. First, half of the metal powder was added to the melted binder and mix for 15-20 minutes. Then, the rest of the powder was added and mixed for 45-60 more minutes. The compounded batch was allowed to cool to 38°C (100°F) and then removed from the mixer and shredded to small particulate. The feedstock contained total of 2wt% binder (agar + glucose) and agar/glucose ratio of 2.2. Spiral testing was conducted on this feedstock composition at two moisture levels.

## CHAPTER 8

### THE FLOW PROPERTIES OF AGAR-GLUCOSE COMPOSITIONS

#### 8.1 Flowability of Composition “A”

The feedstock of composition “A” was divided into two equal portions. The moisture content of the feedstock materials was adjusted to 5.84% (94.16wt% solid) and, 5.2% (94.80wt%). The flow behavior of the materials was evaluated for these moisture levels at 500, 1000, and 1500 psi injection pressures. The material with 5.84% moisture content showed excellent flow properties of  $5.56 \pm 0.63$ ,  $9.89 \pm 0.47$  and  $12.47 \pm 1.34$  inches at applied injection pressures. The feedstock material with 5.2% (94.80wt% solid) only flowed  $2.66 \pm 0.30$  inches at 1500 psi and did not flow at 500 and 1000 psi pressures.

It is shown in previous sections that the flowability of the 17-4PH gas atomized baseline feedstock was diminished completely at 6.7% moisture level (93.3wt% critical solid loading) and minimum moisture level for the material to be moldable was 7.2%. The glucose additive improved the flow characteristics of the feedstock beyond the critical solid loading of the baseline composition. The addition of glucose helped to lower the moisture content by 1.36% and maintained the flowability at proper level.

#### 8.2 Flowability of Composition “B”

The second composition “B” was formulated with agar/glucose ratio of 1 and total binder of 2.8%. The other batch constituents and their amount were kept the same as composition “A”. The same experimental procedure was followed for preparation of this composition. The spiral flow for this composition was evaluated at 5.18% (94.82wt% solid) and 4.96% (95.04wt% solid) moisture levels. The average flow at 5.18% moisture

and at 500, 1000, and 1500 psi injection pressures was  $1.85 \pm 0.26$ ,  $3.04 \pm 0.37$  and  $4.74 \pm 0.16$  inches, respectively. The feedstock material at 4.96% (95.04wt% solid) moisture level totally lost its flowability at 500 psi injection pressure. At higher injection pressures the material demonstrated poor flowability. The average spiral flow was only  $2.70 \pm 0.33$  inches at 1000 psi. and  $3.51 \pm 0.31$  inches at 1500 psi.

### **8.3 Flowability of Composition “C”**

This composition contains an agar/glucose ratio of 0.82 and total of 2.6wt% binder in its batch formulation. The spiral flow properties of this batch were evaluated at 5.51%(94.49wt% solid) and 4.98% (95.02wt% solid) moisture contents. The average flow at 5.51% moisture content was  $5.05 \pm 0.45$ ,  $8.59 \pm 1.45$  and  $9.22 \pm 1.08$  inches at 500, 1000, and 1500 psi injection pressures. The respective average flow at 4.98% (95.02wt% solid) moisture level was  $1.68 \pm 0.08$ ,  $2.56 \pm 0.10$  and  $5.68 \pm 0.24$  inches at applied injection pressures of 500, 1000, and 1500 psi.

### **8.4 Flowability of Composition “D”**

Composition “D” comprises of 2.3wt% binder and agar/glucose ratio of 1. The agar/glucose ratio of this composition is same as composition “B”, but contains 0.5wt% lower binder in its formulation. The spiral flow testing was conducted at 5.50% (94.50wt%solid) moisture content. The material did not flow at 500 psi pressure and had impotent flow at higher injection pressures. The average flow was only  $3.05 \pm 0.13$  and  $5.73 \pm 0.51$  inches at 1000 and 1500 psi respectively.

### **8.5 Flowability of Composition “E”**

This composition was prepared with an agar/glucose ratio of 0.72 and 2.7wt% binder. The moisture content of the feedstock material was adjusted to 5% (95.0wt% solid). The composition “E” did not illustrate sufficient flowability at this moisture level. The material showed an average flowability of  $1.85\pm 0.14$ ,  $3.32\pm 0.28$  and  $6.01\pm 0.28$  inches at 500, 1000, and 1500 psi pressure respectively.

### **8.6 Flowability of Composition “F”**

The feedstock material comprises of 3.4wt% binder and agar/glucose ratio of 0.5. Spiral experiment was conducted at 5.44% (94.56wt% solid) and 5.09% (94.91% solid) moisture contents. The material showed excellent flowability at 5.44% moisture level. The average spiral flow was  $9.68\pm 0.55$  and  $16.60\pm 1.28$  inches at 500 and 1000 psi pressures. The feedstock material was not tested at 1500 psi pressure because of its high flowability. The feedstock illustrated a decent flowability at 5.09% moisture content. The average flow at this moisture level was  $4.55\pm 0.93$ ,  $7.28\pm 0.92$  and  $9.62\pm 0.23$  inches at 500, 1000 and 1500 psi injection pressures.

### **8.7 Flowability of Composition “G”**

This composition was slightly different from composition “F”. The agar/glucose ratio of 0.56 was higher by 0.06 from composition “F”. The feedstock material showed sufficient flowability at lowest moisture contents of 5.0%. However, the total binder was as high as 3.6%. In contrast with composition “F” this material became more responsive to

injection pressures, especially at 1500 psi. The flow distances were  $5.0\pm 0.30$ ,  $8.1\pm 0.21$  and  $10.9\pm 0.18$  inches at 500, 1000 and 1500 psi pressures, respectively.

## **8.8 Results and Discussion**

The addition of glucose in the binder formulation caused the cross-linking of agar gel to detangle and lowered the viscosity of the binder. The low viscosity binder helped to improve the flow properties of the feedstock at higher solid loading. Table 7.1 presents a summary of the compositions and their flow properties. The results clearly show that the addition of glucose in the composition made a significant improvement on flow properties of the 17-4PH feedstock material containing gas-atomized powder. Composition “B” with agar/glucose ratio of 1 and total binder content of 2.8 had a poor flowability at 5.18% moisture. The material lost its flowability at 4.96% moisture level. Composition “D” with same agar/glucose ratio of 1 and 0.5% (total binder 2.3%) lower binder than composition “A” could not be processed at 5% moisture content.

**Table 8.1** Summary of flow characteristics of agar-glucose feedstock compositions for 17-4PH (UFP) gas atomized powder.

Composition	Agar/Glucose Ratio	Total Binder %	% H <sub>2</sub> O	%Solid Binder +Metal	Metal Vol %	Flow Distance (inch) at		
						500 psi	1000 psi	1500 psi
A	2.2	2	5.84	94.16	62.5	5.6	9.9	12.5
			5.20	94.80	64.8	0	0	2.7
B	1	2.8	4.96	95.04	63.7	0	2.7	3.5
			5.18	94.82	62.9	1.9	3.0	4.7
C	0.82	2.6	4.98	95.02	64.1	1.7	2.6	5.7
			5.51	94.49	62.2	5.1	8.5	9.2
D	1	2.3	5.00	95.00	64.8	Could not be fed at this solid loading		
			5.50	94.50	63.0	0	3.1	5.7
E	0.72	2.7	5.01	94.99	63.8	1.9	3.3	6.0
			---	---	---			
F	0.50	3.4	5.09	94.91	61.8	4.6	7.3	8.6
			5.44	94.56	60.6	9.7	16.6	---
G	0.56	3.6	5.00	95.00	61.7	5.0	8.1	10.9
			---	---	---			
Baseline	NA	2.1	7.30	92.70	57.4	3.6	8.1	11.4
			6.70	93.30	59.3	0	0	0

At higher moisture level of 5.50% the material did not flow at 500 psi and had an indigent flow at 1000 and 1500psi injection pressures. Comparing composition “E” with

“B” and “C” indicates that the material flowability at about 5% moisture content has a tendency to improve as the agar/glucose ratio is reduced to 0.72.

Composition “F” with agar/glucose ratio of 0.50 and 3.4% binder showed decent flowability at 5.09% moisture content. In comparison with composition “E” it is indicated that lowering the agar/glucose ratio to 0.5 and increasing the binder content to 3.4% improved the flowability at 5% moisture level from 1.9 to 4.6 inches at 500psi applied injection pressure.

Composition “G” formulated with 3.6% binder and agar/glucose ratio of 0.56, which are slightly higher than composition “F”. In comparison with composition “F” composition “G” showed better flowability especially at 1500 psi pressure. This composition contains lowest moisture content of 5% and highest binder amount of 3.6%. The lower moisture content facilitates shorter drying cycle for the molded articles.

Composition “A” contains highest agar/glucose ratio of 2.2. It has lowest binder content of 2%. The binder system comprises of 31% glucose and 69% agar powder. This composition with 5.84% has an optimum moisture content with lowest binder amount compared to other compositions in Table 8.1 except, the baseline composition. This composition demonstrated the best flowability at applied injection pressures. It also contains the highest metal loading of 62.50vol%. This composition has the potential for reducing the overall cost of the feedstock material, since 31% of the total binder is glucose (\$3.96/lb), which, is 66.3% cheaper than agar (\$11.75/lb) powder.

The results show that two best compositions are composition "A" and "G". Each of these compositions has its advantages and disadvantages. Some of the advantages of composition “A” are low binder content, lower binder costs, high metal content of

62.50vol%, and excellent flow properties. The disadvantage is the 5.84% moisture contents, which prolongs the drying cycle of molded articles prior to sintering process. Storing the feedstock material of this composition in a closed container had the tendency to develop slight moisture condensation on the wall of the container (Rainforest effect). This requires the incorporation of the condensed moisture with the feedstock material prior to usage by tumbling the container. In contrast with baseline feedstock, composition “A” significantly enhanced the metal solid loading from 57.1 to 62.5vol% and lowered the required moisture in the composition by 1.5%.

The advantages of composition “G” are very low moisture content of 5.0%, good flow properties and no rainforest effect. The disadvantage is the high binder content of 3.6%. However, composition “G” considerably improved the baseline feedstock formulation of 17-4PH (UFP) feedstock. The metal loading increased by 4.3vol% and moisture content reduced by 2.3%.

### **8.9 Effect of Solid Loading on Molded Weight**

Feedstock material with high solid loading plays an important role on improving as-molded weights, green density, better dimensional control and lowering the final shrinkage of molded articles. The as-molded weight of the parts increased as the solid loading increased. Since the volume of the cavity is constant the green density is directly effected by the green weight. To study the effect of solid loading on as-molded weight (green weight) and green density, several experiments were conducted on feedstock material with composition “G”. A batch of feedstock material with “G” recipe was prepared. The material was divided in two equal portions. The moisture content of the

materials was adjusted to 5.46% (94.54wt% solid, 60.1vol% metal) and 5.0% (95.0wt% solid, 61.7vol% metal). Eleven tensile bars were molded at each solid level to evaluate the effect of solid loading on as-molded weights and green density.

The tensile bar samples were molded using 55 tone Cincinnati Milacron injection molding machine. The samples were molded at 600 psi injection pressure, 300 psi holding pressure, 3 second holding time and 0.5"/sec injection speed. The mold temperature was maintained at 77°F (25°C). Figure 8.1 shows the tensile bar mold cavity and the cavity dimensions of the mold.

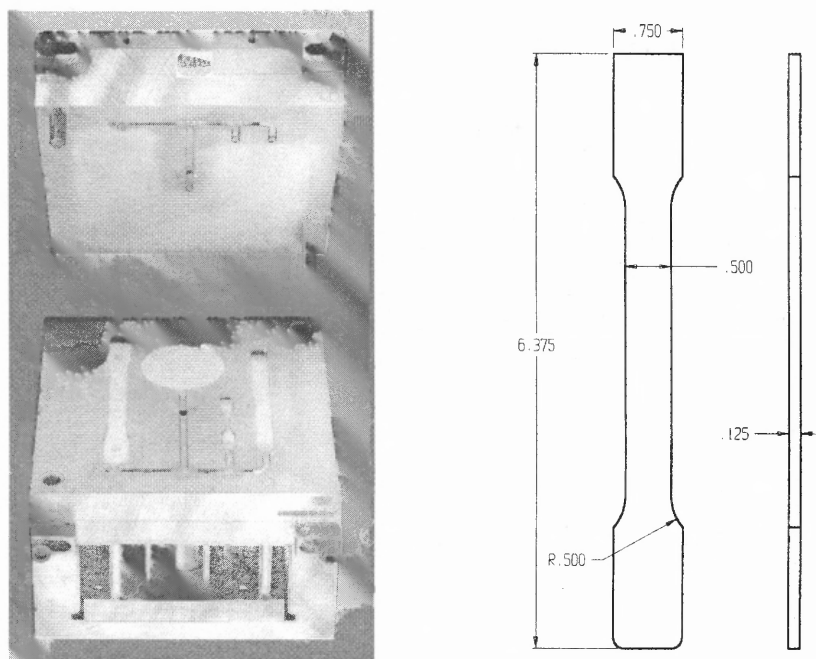


**Figure 8.1** Shows the tensile bar mold and the cavity dimensions of the mold.

Figure 8.2 presents the weight variation of samples molded with 17-4PH (UFP) gas atomized feedstock material with 5.46 and 5.0% moisture contents. The average as-molded weight of the tensile bars with 5.46% moisture content was  $42.66 \pm 0.07$  grams.

The average green density of the samples was calculated to be  $5.36 \pm 0.01 \text{ g/cm}^3$  by dividing the average green weights to  $7.96 \text{ cm}^3$  ( $0.49 \text{ in}^3$ ) the volume of the mold cavity. The average weight with 5.0% moisture was  $43.18 \pm 0.09$  grams and average green density determined to be  $5.43 \pm 0.01 \text{ g/cm}^3$ . The result indicates that reducing the moisture content by 0.46% enhanced the as-molded weight by 1.2%.

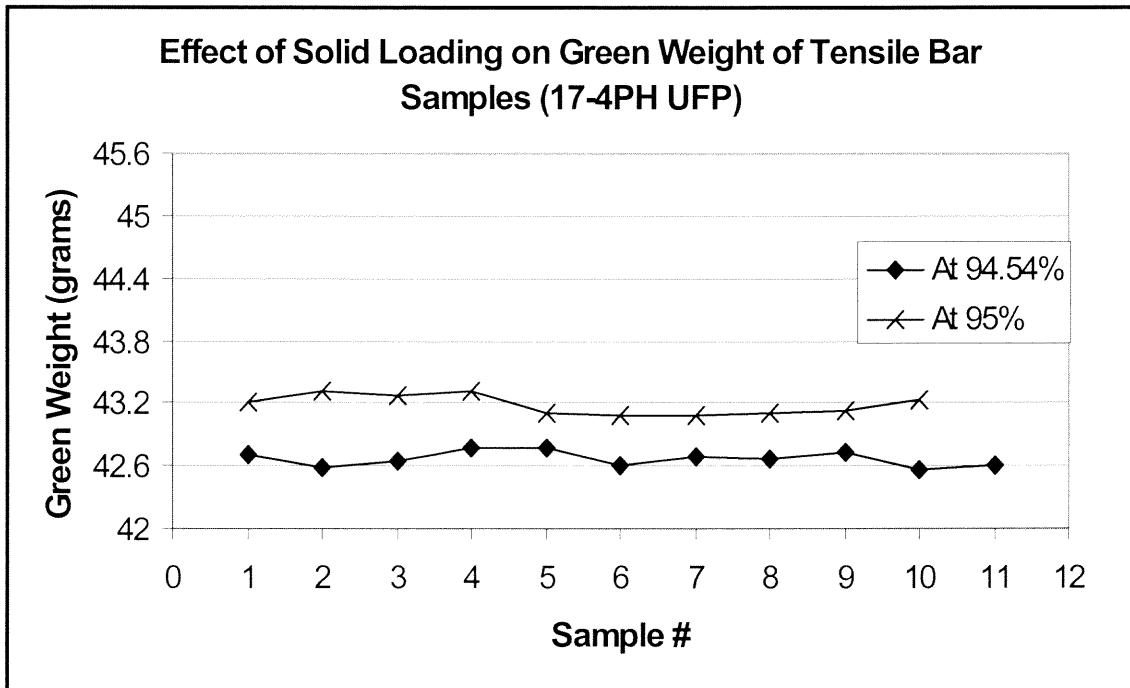


**Figure 8.2** Effect of solid loading of 17-4PH (UFP) materials on as molded weighs of tensile bar samples.

## CHAPTER 9

### FEEDSTOCK CONTAINING 17-4PH ATMIX POWDERS

#### 9.1 Study the Effect of Additives on 17-4PH (Atmix) feedstock

In this section, the effect of three additives on flow properties of feedstock material containing 17-4PH water atomized (Atmix) powder was investigated. These additives were glucose, sucrose and fructose. The maximum and critical solid loading of feedstock containing water- atomized powder was evaluated. The experimental formulations for the feedstock using this powder was that of composition “G” and “A” which generated good results for gas atomized powder. This way the effect of different powders on the rheology of the feedstock can be compared.

#### 9.2 Glucose Additives

An experimental batch of feedstock using water atomized 17-4PH supplied by the Atmix company was compounded using 3.6% binder and 0.56 agar/glucose ratios. This formulation is the same as composition “G” applied to gas atomized powder described in the previous chapter. For the water atomized formulation, the nomenclature “G<sub>w</sub>” will be used. The batch was prepared with 7842g of stainless steel 17-4PH (Atmix) water atomized powder, 100g of agar (TIC100), 180g of glucose (CH<sub>2</sub>OH(CHOH)<sub>4</sub>CHO), and 680g of DI/H<sub>2</sub>O. A mixture of 1.6 g of Methyl-p-hydroxybenzoate and 1.2 g of Propyl-p-hydroxybenzoate was added to the batch as an anti fungal agent. The batch preparation steps and conditions were identical to that of the gas atomized feedstocks.

The feedstock material was divided in three portions and the moisture contents adjusted to 5.98% (94.02% solid), 5.5% (94.50% solid) and 5.0% (95.0% solid). The

spiral flow experiments were conducted on the feedstock material at these moisture levels. The feedstock material with 5.98% (94.02%solid) moisture content showed excellent flow properties. The average flow was  $4.42\pm 0.20$ ,  $9.82\pm 0.37$  and  $19.54\pm 1.57$  inches at 500, 1000, and 1500 psi, injection pressure respectively. The results also showed that the material became more responsive to flow at higher shear. When the injection pressure changed from 1000 to 1500 psi, the flow increased significantly from 9.82 to 19.54 inches.

The flowability of the feedstock declined drastically at 5.5% (94.50% solid) moisture level. However, it still showed sufficient flowability for processing. The average flow measure to be  $2.54\pm 0.20$ ,  $5.60\pm 0.18$  and  $9.35\pm 0.26$  inches. Lowering the moisture level by 0.48% degraded the flowability by more than 42% at 500 and 1000 psi and about 52% at 1500 psi pressures. At 5.0% (95.0% solid), moisture content the feedstock material became very difficult for processing and eventually jammed the injection molding machine. The material at this moisture content is considered unusable.

### 9.3 Sucrose Additive

The effect of sucrose ( $C_{12}H_{22}O_{11}$  from Alfa Co.) on flow properties of 17-4PH (Atmix) feedstock material was evaluated. An experimental batch with this additive was prepared. The batch compounded using 6400g 17-4PH (Atmix) powder, 81.6g agar (TIC100), 146.9g sucrose, 600g H<sub>2</sub>O, 1.2g methyl-p-hydroxybenzoate and 1g propyl-p-hydroxybenzoate. This batch comprises of 3.6% binder (agar + sucrose) and agar/sucrose ratio of 0.56 (same as composition “G<sub>w</sub>”). The moisture content of the feedstock was adjusted to 6.0% (94% solid). The flow distance of the material at 500psi injection

pressure was only  $2.12 \pm 0.15$  inches. The flow distances were  $5.62 \pm 0.73$  and  $10.82 \pm 0.97$  inches at 1000 and 1500 psi pressure respectively. The feedstock material at 5.5% (94.5% solid) moisture content did not flow at 500 psi and the flow was insignificant at higher pressures. Thus, it appears that the sucrose degraded the flow properties compared to the agar only binder.

#### **9.4 Fructose Additive**

A batch of 17-4PH (Atmix) materials was prepared with fructose ( $C_6H_{12}O_6$  from Alfa Co.) additive. The feedstock material was compounded with an agar/fructose ratio of 0.56 and 3.6% binder. Spiral flow experiment conducted at 6% (94.0% solid) moisture content. At this moisture level, the material was very difficult to be fed effectively into the injection molding machine. Also, the material did not demonstrate any flowability at applied injection pressures. The addition of fructose did not provide any advantages. Fructose, like sucrose, degraded the flow properties compared to agar only binder.

#### **9.5 Results and Discussion**

The addition of glucose ( $CH_2OH(CHOH)_4CHO$ ) as a part of the binder system was effective in changing the rheology of the 17-4PH (Atmix) feedstock material. The 17-4PH (Atmix) feedstock with agar/glucose ratio of 0.56 and total binder of 3.6% showed good flowability. The spiral experiments were conducted on water-atomized feedstock at 5.98% (94.02% solid), 5.5% (94.50% solid) and 5.0% (95.0% solid) moisture content. The flowability of the material at 5.98% (94.02% solid) was  $4.42 \pm 0.20$ ,  $9.82 \pm 0.37$  and  $19.54 \pm 1.57$  inches at 500, 1000, and 1500 psi injection pressure respectively. Excessive

flow was observed at this moisture level, especially at higher shear rate (1500 psi injection pressure). The material could not be fed into the injection molding machine at 5.0% (95.0% solid) moisture level because of high viscosity due to low moisture content. The best result in terms of moisture content and flowability was achieved at 5.5% (94.50% solid) moisture level. The material at this moisture level demonstrated a flow of  $2.54 \pm 0.2$ ,  $5.60 \pm 0.18$ , and  $9.35 \pm 0.26$  inches at 500, 1000, and 1500 psi injection pressures.

It is shown that the same binder formulation developed for gas atomized powder feedstock effectively improved the flow properties of the water atomized powder. Applying the “G<sub>w</sub>” formulation significantly improved the solid loading of the water-atomized feedstock. However, the material could not be processed at 5.0% (95 wt% solid) moisture content while the gas atomized feedstock with the same formulation molded at this moisture level. This is very well related to the morphology and characterizations of these powders i.e. angle of repose, particle shape and size distributions, which were discussed in previous chapters.

Using a sucrose additive did not show significant advantages. The feedstock material with “G<sub>w</sub>”(agar/sucrose of 0.56 and total binder of 3.6wt%) formulation containing sucrose tested at 6% (94.0wt% solid). The average flow at 500 psi was  $2.12 \pm 0.15$  inches, and  $5.62 \pm 0.73$  and  $10.82 \pm 0.97$  inches at 1000 and 1500 psi injection pressures. The flowability of the material at 5.5% (94.5wt% solid) moisture content was zero at all applied pressures. This additive was not effective at solid loading higher than 94wt%. Replacing sucrose with fructose in the feedstock formulation deteriorated the flowability of the material. The feedstock material at 6.0% (94.0wt% solid) moisture was

very difficult to be processed and showed no flowability. Figure 9.1 shows the effect of these additives on flowability of 17-4PH (Atmix) feedstock materials.

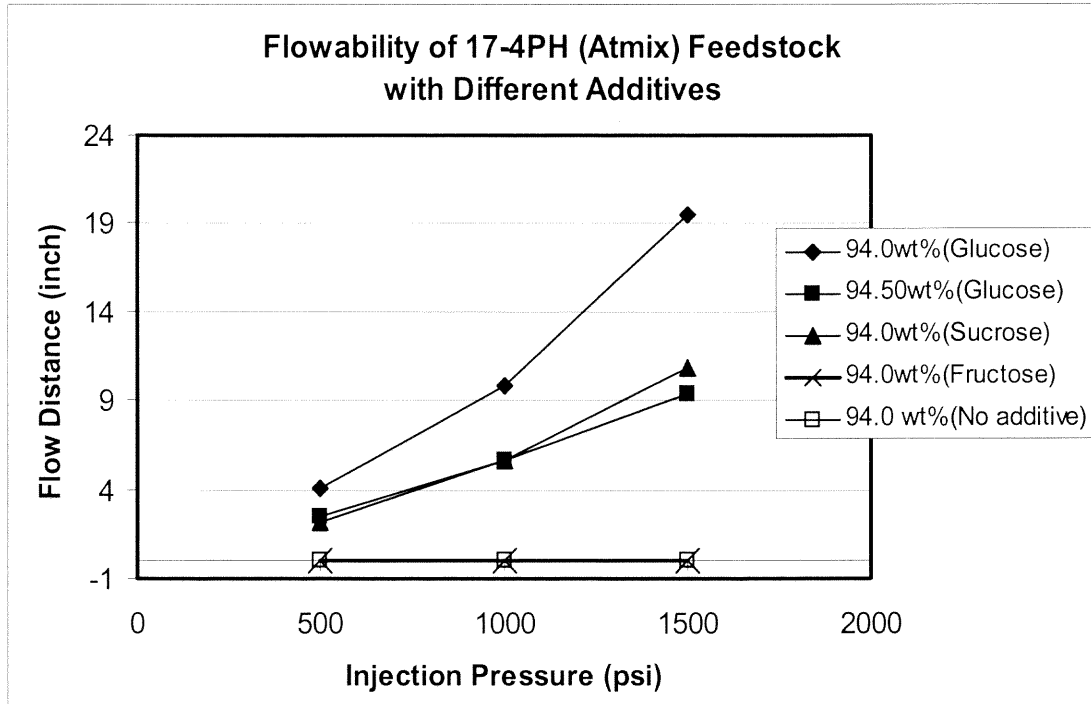


**Figure 9.1** Effect of different additives on flowability of 17-4PH (Atmix) feedstock

The best result with water atomized powder and glucose additive was achieved using “G<sub>w</sub>” composition at 5.5% moisture level. The material with 5.98% moisture had excess flowability, and material with 5.0% was unusable due to lack of flow.

### 9.6 Effect of Solid Loading on As-Molded Weight

A batch of 17-4PH (Atmix) feedstock material compounded using “G<sub>w</sub>” formulation. The material was molded at 6% (94wt% solid) and 5.45% (94.55wt% solid) moisture levels. Thirty rings samples were molded at 6% (94wt% solid) moisture level to monitor

the as-molded weight variation and determine the average weight of the samples. The cooling time was set for 50 second (from end of injection time to the time mold is open) for molding these samples.

Twenty-five additional samples were molded using 30, 20 and 15 second to find the minimum applicable cooling time. The samples with 15 seconds cooling time were not sufficiently solidified and tend to stick to the mold cavity upon removal. With 30 and 20 seconds cooling time, the samples could be remove from the mold cavity with no difficulty. Therefore, the minimum cooling time was determined to be 20 seconds.

Thirty samples were molded with the feedstock material containing 5.45% (94.55wt% solid) moisture. The cooling time was set for 50 seconds for molding the parts. The as-molded weight variation and average weight of the parts was compared with samples molded at 6% (94wt% solid) moisture content. The minimum cooling time for the parts was found to be 15 seconds. Lesser cooling time was found to be insufficient. Figure 9.2 shows a run chart for samples that were molded at 6% (94wt% solid) and 5.45% (94.55wt% solid) moisture levels.

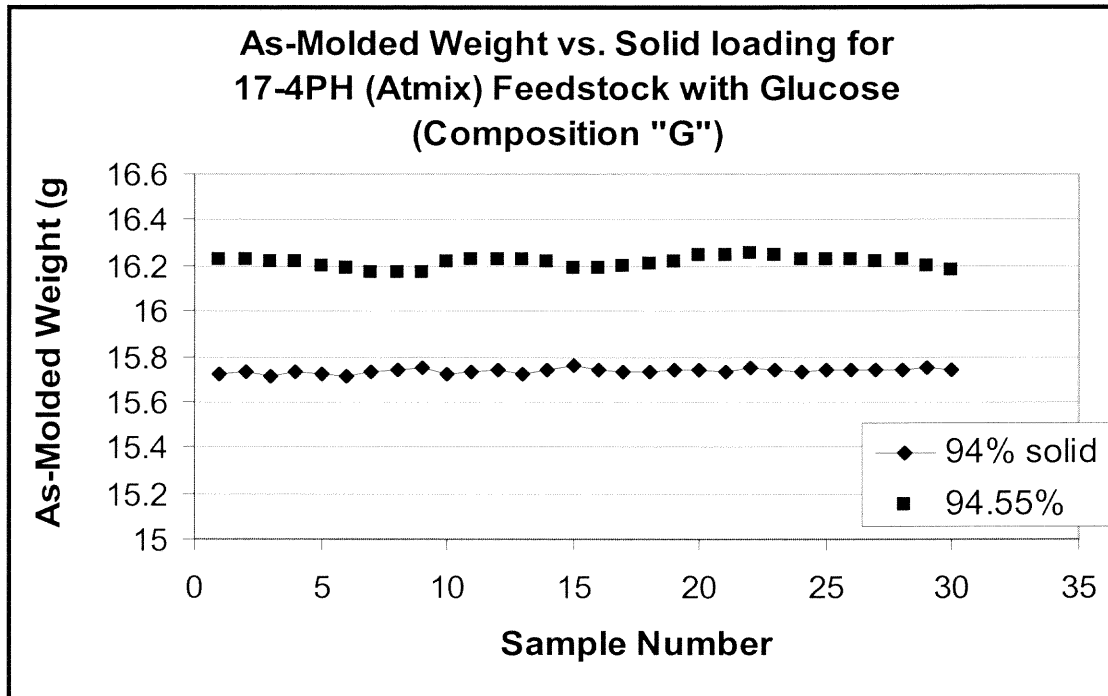


**Figure 9.2** Weight variation of as-molded parts using 17-4PH (Atmix) feedstock containing glucose additive (composition “G<sub>w</sub>”)

**Table 9.1** Summary of the molding results for 17-4PH (Atmix) composition “G<sub>w</sub>”

Feedstock Composition	%Moisture (Wt% solid)	Average As-molded weight (g)	Minimum cooling time (sec.)	Agar/Glucose ratio & Total binder%
Baseline	8.0 (92.0)	15.13 ±0.028	30	-----, 2.1
G <sub>w</sub>	6.0 (94.0)	15.73±0.012	20	0.56, 3.6
G <sub>w</sub>	5.45 (94.55)	16.21±0.023	15	0.56, 3.6

Comparing with the baseline composition, the addition of glucose in the feedstock formulation improved the as-molded weight of the samples by about 7.1% and reduced the cooling time by 50%. The average as-molded weights also increased by about 3% as

the moisture content of the feedstock containing glucose reduced from 6.0% to 5.45%. The cooling time improved by 25%.

### 9.7 Composition “A” containing 17-4PH (Atmix) Powder

It was shown that composition “A” (agar/glucose ratio of 2.2 and total binder of 2wt%) could produce a feedstock material having the highest atomized metal powder content for the gas-atomized powder used. Three experimental batches were compounded with this composition using water atomized 17-4PH (Atmix) powder to evaluate the maximum and critical solid loading of this formulation in water atomized powder. The batch composition was identified as “A<sub>w</sub>” which stands for the composition “A” containing water atomized metal powder. The moisture content of these batches was adjusted to 6.69% (93.31% solid), 6.49% (93.51% solid) and 6.0% (94% solid). The moldability of this formulation was evaluated by molding more than 40 tensile bar specimens using 55 tons Cincinnati injection molding machine. The feedstock material at 6.69% (93.31% solid) and 6.49% (93.51% solid) moisture levels was molded with no difficulty. However, the material with 6.0% (94% solid) moisture content completely lost its moldability. Consequently, the maximum and critical solid loading for this formulation was identified as 93.51wt% and 94.0wt% respectively.

Figure 9.3 shows the as-molded weight variation of tensile bar samples molded at 6.69% (93.31% solid) and 6.49% (93.51% solid) moisture levels. The average as-molded weight of 46 samples molded at 93.31wt% solid was  $41.40 \pm 0.046$  grams. The average weight for the samples molded at 93.51wt% solid was  $41.66 \pm 0.041$  grams. A summary of the molding results for “A<sub>w</sub>” feedstock formulation is shown in Table 9.2.

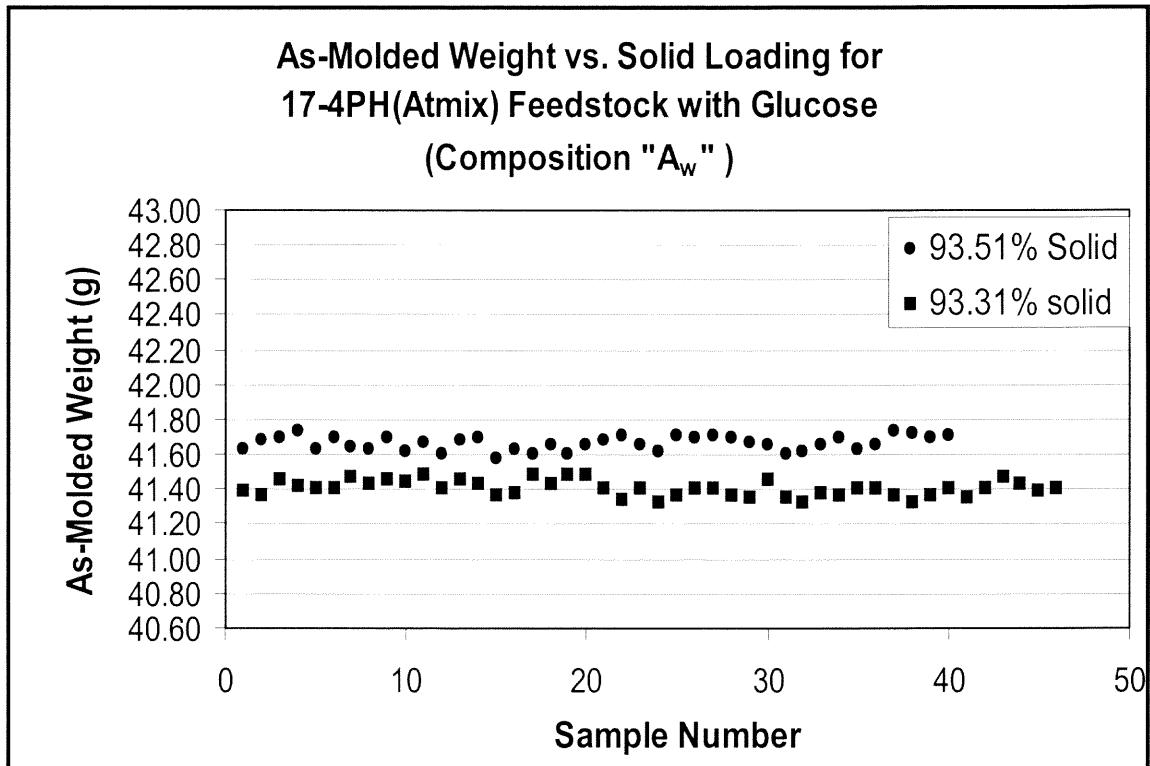


**Figure 9.3** Weight variation of as-molded parts using 17-4PH (Atmix) feedstock containing glucose additives (composition "A<sub>w</sub>")

**Table 9.2** Summary of the molding results for 17-4PH (Atmix) composition "A<sub>w</sub>"

Feedstock Composition	%Moisture (wt% solid)	Average As-molded weight (g)	Agar/Glucose ratio & Total binder%
A <sub>w</sub>	6.69 (93.31)	41.40±0.045	2.2, 2.0
A <sub>w</sub>	6.49 (93.51)	41.66±0.041	2.2, 2.0

## 9.8 Results and Discussion

It was shown in previous sections that the maximum solid loading for the baseline composition comprising of 17-4PH (Atmix) water atomized powder was 92.7wt% (7.3% moisture). The effect of glucose, sucrose and fructose additives was evaluated for enhancing the solid loading of the feedstock material containing water-atomized powder. The effect of sucrose was not significant and fructose additive did not provide any advantages. However, the glucose additive improved the properties of the feedstock material by increasing the amount of metal loading while still maintaining useful flow.

Two formulations “G<sub>w</sub>” and “A<sub>w</sub>” were employed to incorporate the glucose additive in the feedstock material. Both formulations significantly increased the solid loading of the feedstock. The maximum solid loading of 94.50wt% (5.50wt% moisture) was achieved with G<sub>w</sub> (agar/glucose ratio: 0.56 and total binder: 3.6wt%) formulation. The maximum metal powder content was 59.90vol%.

The material with A<sub>w</sub> (agar/glucose ratio: 2.2 and total binder: 2wt%) formulation was molded at 93.51wt% solid (6.49wt% moisture). This solid loading is about 1wt% lower than the G<sub>w</sub> formulation and, contains 1wt% more moisture. However, this formulation improved the maximum metal powder content by 0.3vol% (60.20vol%). Table 9.3 presents a summary for both formulations.

**Table 9.3** Summary and results of agar-glucose formulations for 17-4PH (Atmix) water atomized powder

<b>Composition</b>	<b>Agar/Glucose Ratio</b>	<b>Total Binder %</b>	<b>% H<sub>2</sub>O</b>	<b>%Solid Binder + Metal</b>	<b>Metal powder Vol%</b>	<b>Max. Solid Loading</b>	<b>Critical Solid Loading</b>
<b>A<sub>w</sub></b>	2.2	2	6.49	93.51	60.20	93.51 wt%	94.0 wt%
<b>G<sub>w</sub></b>	0.56	3.6	5.50	94.50	59.90	94.50 wt%	95.0 wt%

Both of these formulations significantly improved the rheology of the material compared with the baseline, which resulted in the increase of the solid loading of the feedstock. The advantage and disadvantage of these formulations should be evaluated from several points of view, cost saving, effects on final shrinkage, microstructure and final chemistry of the material after sintering. Except for the cost evaluation the other issues will be investigated in later sections.

The addition of glucose significantly reduced the cost of the binder. Agar powder is the most expensive constituent of the binder system (about \$23.50/kg). The glucose powder is about 1/3 of the agar's cost (\$8.40/kg). Replacing the portion of the binder with glucose can reduce the cost of the binder. The binder composition for the "G<sub>w</sub>" formulation comprises of 36% agar and 64% glucose. Substituting 64% of the total binder with glucose reduced the cost of the baseline binder by 42.4%. Even though this composition contains 1.6wt% more binder than the baseline formulation, the cost saving remains significant. The binder system for "A<sub>w</sub>" formulation contains 68.75% agar and 31.25% glucose. This formulation reduced the cost of the baseline binder by 20.6%. It was shown that feedstock material produced with "A<sub>w</sub>" formulation contains highest metal powder content. The lowest binder cost was achieved with this formulation.

## CHAPTER 10

### THE SINTERING PROCESS

#### 10.1 Debinding

Debinding is a very critical primary step between molding and sintering where, the binder is extracted by heat, solvent or other techniques. The process of removing the binder and other contamination prior to sintering temperature has a significant effect on final chemistry, density and properties of a part. This step in polymer binder system controls the part size and thickness limitation. The total removal of the binder becomes very difficult and economically infeasible as the part size and thickness increases. Long debinding time and cracking are among major obstacles for this binder system. The debinding process has been considered the most critical step in powder injection molding (PIM) because of the long time needed to burn out the binders without introducing defects such as blistering, warping, and skin exfoliation [33]. A major limitation on the processing of ceramics by injection molding is the long time taken to burn out the polymeric binder [34]. A 3mm thick Injection molded aluminum test bar samples containing polypropylene-based binder system required 28 hours debinding time in air and nitrogen to completely remove the binder [35]. The effect of doubling the section thickness to 6mm was an increased of the debinding time by 3.6 times (about 100 hr.). The debinding process commonly conducted in a separate furnace. The debinded parts are then transferred to a sintering furnace to complete the densification process. In contrast, for the agar binder system debinding is followed by sintering in the same furnace. An agar-based sample with 2.5cm thickness could be debinded within 30 to 45 minutes at 250-300°C.

## 10.2 Sintering

Sintering or densification is an irreversible thermodynamic phenomenon to convert unstable packed powder having excess free energy to stable sintered agglomerates [36]. The process involves the fusion of particles, volume reduction (shrinkage), decrease in porosity, and increase in grain size. Sintering is a high temperature consolidation process that usually takes place at close to the melting temperature of the material. Sintering time, temperature, as well as sintering atmosphere, heating rates, material composition and powder particle size plays an important role in this process. The process creates strong bonding between the particles and enhanced the density and mechanical properties of the material. The following criteria must be met before sintering can occur [37]: a) A mechanism for material transport must be present; b) A source of energy to activate and sustain this material transport must be present. The primary mechanisms for transport are diffusion and viscous flow. Heat is the primary source of energy, in conjunction with energy gradients due to particle-particle contact and surface energy. Reed [38] explains that the driving force for sintering compacted ceramic particles is due to the reduction in the total free energy  $\Delta G_T$  of the system

$$\Delta G_T = \Delta G_v + \Delta G_b + \Delta G_s \quad (10.1)$$

Where  $\Delta G_v$ ,  $\Delta G_b$ , and  $\Delta G_s$  represent the change in free energy associated with the volume, boundaries, and surfaces of the grains, respectively. The major driving force in conventional sintering is  $\Delta G_s$  but the other terms may be significant in some stages for some material system.

The sintering process has been divided in three main stages, initial, intermediate and final [37]. During the initial stage, neck is forming at the contact point of particles. At the intermediate stage neck growth, pore rounding and elongation occur. Density increases significantly at this stage. In the final stage, grains continue to grow, the number of pore decreases and final densification transpires. A combination of several mass transport mechanisms such as grain boundary, surface and volume diffusions, plastic flow and evaporation condensation could take place during the sintering stages. Figure 10.1 shows the alternative paths for the atoms to form bonding during the first stage of sintering [39].

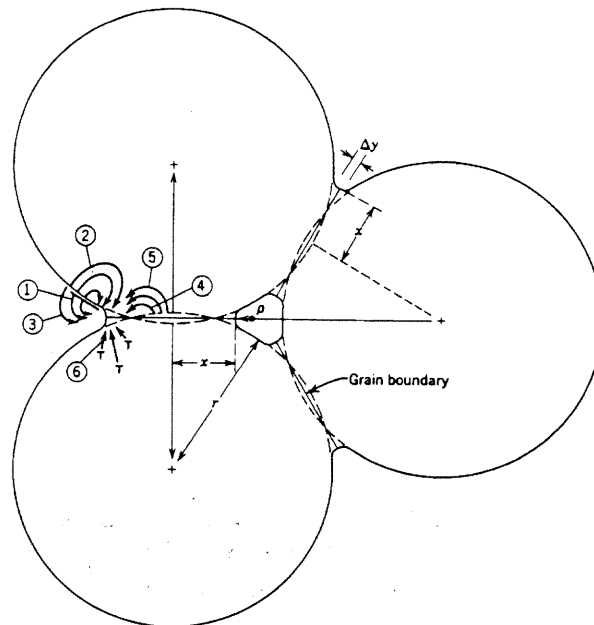


**Figure 10.1** Alternative paths for matter transport during the initial stages of sintering. Courtesy M. A. Ashby.

The kinds of changes that may occur during sintering are illustrated in Figure 10.2 [37][39]. The contacted particles were fusing together and the shape of the pore between them is changed. Dimensional changes or shrinkage ( $\Delta L_0$ ) also occurred.

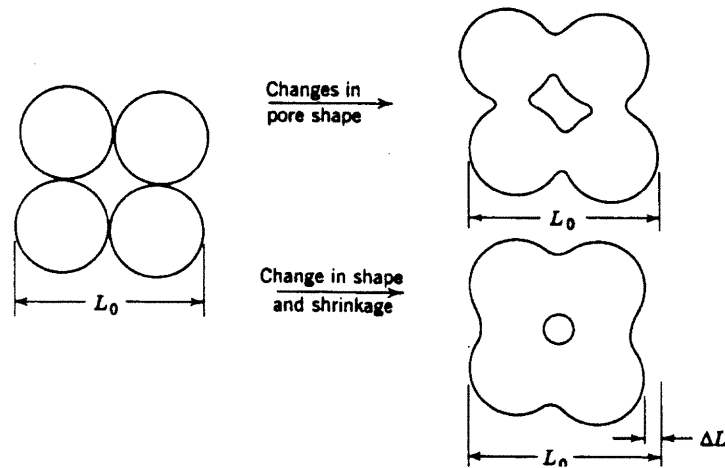


**Figure 10.2** Change of pore shape and dimensional changes during sintering process.

Shrinkage, is a decrease in physical dimensions of a particulate compact, occurs during sintering. Shrinkage is sensitive to sintering time and temperature. By extending the sintering time, it is possible to reduce the process sensitivity to small fluctuation [40]. It is indicating that errors in sintering time have less influence on final dimensions. The effect of sintering temperature is much larger; there is more shrinkage at higher temperature. Figure 10.3 shows the effect temperature and time on dimensional shrinkage [40]. Sintering shrinkage increases exponentially with temperature. Therefore, at higher temperature a small change leads to a greater dimensional variation. Sintering

shrinkage is less sensitive to time. As the time progresses, there is less change in shrinkage.

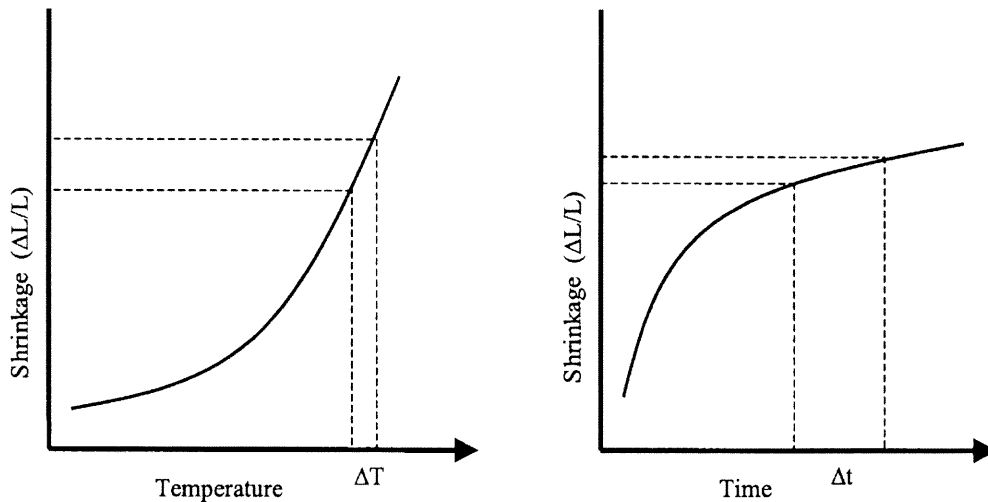


**Figure 10.3** Influence of the sintering temperature and sintering time on linear shrinkage.

Various sintering conditions have been developed and employed for sintering different types of alloys. The specific details of the repeatable successful sintering conditions have been kept as proprietary practices. The sintering atmosphere is an important contributor in a sintering process. Some of the common types of sintering atmosphere are; air, vacuum, inert gases, hydrogen and combination of two or more. Exner [41] studied the effect of nitrogen, air, hydrogen, argon and mixture of 25% nitrogen and 75% hydrogen on sintering of stainless steel powder. The level of sensitivity to sintering atmosphere varies with different materials. For stainless steel

alloys, the sintering atmosphere should be selected and controlled carefully to hold the final oxygen and carbon content to a desirable level.

The sintering of 17-4PH samples was conducted in a nine cubic feet Elnik batch furnace. The samples molded with baseline composition as well as “A” and “G” compositions were sintered under the same sintering conditions. The following sintering conditions were employed for sintering tensile bar samples molded with 17-4PH feedstock materials. At the initial stage, the samples were held at 110 °C for 1 hour in air to remove any residual moisture. The temperature was raised to 320 °C and held for 4 hours in air. The binder content is eliminated at this stage. The debinding followed by vacuum pump down and then introducing hydrogen gas into the furnace. Temperature was raised to 1010 °C and held for 1 hour then followed by 1365 °C and 2 hours soaking. At the final stage, the furnace temperature was ramped down at 5 °C/min. to room temperature.

### **10.3 Shrinkage Prediction and Measurements**

The starting dimensions of molded part changes during the sintering process and all final dimensions become smaller than the green part dimensions. This dimensional change has the potential to be a source of part distortion and cracking. Reducing the sintering shrinkage helps to eliminate the sources for these defects and provides better control on dimensional tolerances. Shrinkage is inversely effected by volume percent of the metal powder in the feedstock (lower binder content). This provides more particle contacts and higher packing during molding.

A shrinkage prediction model, based on conservation of mass, has been developed to guide work on a shrinkage adjustment and compound development. The shrinkage was calculated based on the initial volume percent of metal content of the compound at the time of molding and final density of the sintered part. Shrinkage and density are interrelated. Higher sintered density is associated with higher shrinkage for a given solids loading and green part pack profile. Figure 10.4 shows the effect of volume percent of metal content and final sintered density on shrinkage. For comparison, the actual data are shown on the model with open symbols.

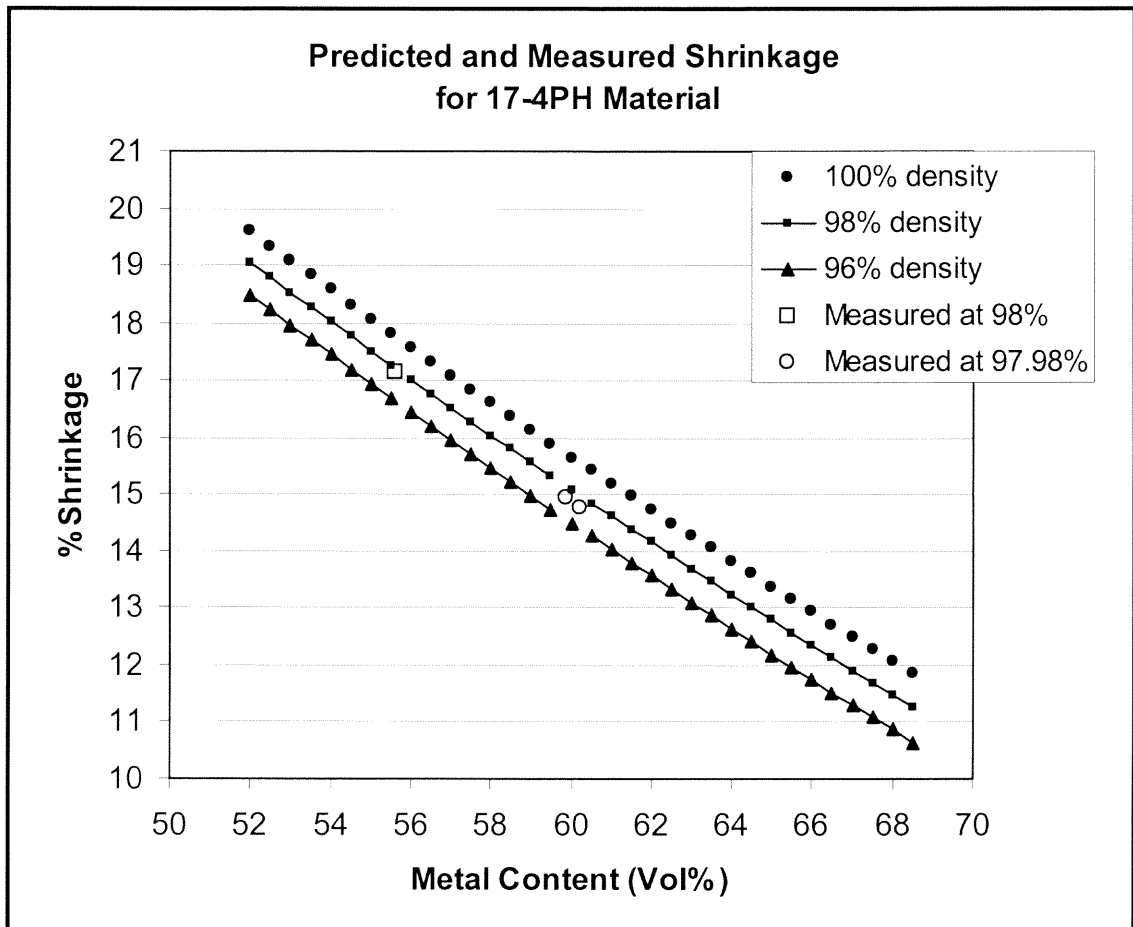


**Figure 10.4** Shrinkage model predictions and data for 17-4PH compounds

Two generalizations based on this model are (1) a 1% increase in volume percent of metal content decreases the final shrinkage by about 0.47%, (b) a 1% decreases in sinter density causes about 0.28% decrease in shrinkage.

The effect of feedstock composition on final shrinkage was evaluated. Tensile bar samples molded with baseline, “A” and “G” compositions and sintered at 1365 °C for 2 hours in hydrogen atmosphere. The percent shrinkage was calculated by comparing the sintered dimensions to the mold dimensions ( $\Delta L/L_0$ ). The density of the sintered samples evaluated using Archimedes’ principle. Table 10.1 presents the effect of the feedstock formulation on the final shrinkage of the tensile bar samples.

**Table 10.1** The effect of feedstock formulation on shrinkage (tensile bar samples)

Compositions	Vol% of Metal	Wt% Solid (metal+binder)	%TD	%Shrinkage (Length)
Baseline (Atmix)	55.6	92.08	98.00	17.15 ±0.02
“G <sub>w</sub> ”	59.9	94.55	97.98	14.95 ±0.20
“A <sub>w</sub> ”	60.2	93.50	97.98	14.76 ±0.13
Baseline (UFP)	57.7	92.79	98.30	16.12 ±0.01
“G”	61.7	95.00	98.50	13.63 ±0.25

In the case of water atomized (Atmix) powder, an average low shrinkage of 14.76 ±0.13 resulted using “A<sub>w</sub>” feedstock formulation. The lowest shrinkage of 13.63 ±0.25 was obtained with “G” formulation containing gas atomized (UFP) powder.

The microstructure of sintered samples of baseline composition containing gas and water-atomized powder were compared with the samples made with “G” composition (containing glucose). The addition of glucose had no effect on microstructure of the sintered samples. On the other hand, the experimental observation indicated that increasing the glucose in the binder formulation reduced the green strength of the as-molded samples. This was noticed in samples molded with composition “G” which had higher glucose content. The as-molded tensile bars with this composition were more susceptible to break or damage during the removal from the mold cavity.

Carbon and oxygen content in the sintered 17-4PH materials have significant effect on mechanical and corrosion properties of this material. These elements react with chromium and deteriorate the corrosion resistance of the sintered parts. The level of these elements has to be controlled within a certain specification (0.07% max. carbon and max. 0.1% oxygen) to insure the final properties. The carbon and oxygen content of the as molded bodies are high due to presence of oxide impurities and binder content in the 17-4PH feedstock. The concentration of both elements must be reduced to an acceptable level in the sintered product. The selection of sintering atmosphere and sintering temperature profile becomes very critical for achieving final concentration of these elements. Table 10.2 shows the carbon and oxygen content of the as molded and the sintered samples.

**Table 10.2** Carbon and oxygen content of 17-PH before and after sintering

Composition of 17-4PH material	As-molded		Sintered		Binder Content (wt%)
	C%	O%	C%	O%	
Baseline	0.808	0.997	0.008	0.044	2.1 (agar only)
G <sub>w</sub>	1.579	2.558	0.240	0.012	3.6 (agar+glucose)
A <sub>w</sub>	--	--	0.008	0.38	2.0 (agar+glucose)

These samples molded with baseline, “G<sub>w</sub>” and “A<sub>w</sub>” compositions were sintered under the standard sintering conditions (see previous section for details). After sintering, the carbon and oxygen concentration in the baseline composition are in the acceptable range of 0.008, and 0.044wt% respectively. However, compositions “G<sub>w</sub>” and “A<sub>w</sub>” responded differently under standard sintering conditions. The final carbon content (0.240 wt%) in composition “G<sub>w</sub>” was higher than specification limit but the oxygen content was (0.012 wt%) within the limit. In the case of composition “A<sub>w</sub>”, the oxygen content (0.38 wt%) is about four times greater than the maximum allowable limits. In contrast, its carbon content (0.008 wt%) is in the adequate range. The results show that the standard sintering conditions is not a desirable setting for sintering composition “G<sub>w</sub>” and “A<sub>w</sub>”. It is suggested that different sintering conditions should be developed for these compositions to meet the proper carbon and oxygen content in the sintered parts.

## CHAPTER 11

### CONCLUSIONS

#### 11.1 Concluding Remarks

This study shows that increasing the volume fraction of the metal powder in the feedstock formulation has significant effect on lowering the final shrinkage of the sintered articles. For this purpose, the effect of several factors was investigated.

1) Two types of metal powder, 17-4PH (Atmix) water atomized and 17-4PH (UFP) gas atomized were evaluated for high solid loading feedstock formulation. The particle size and shape of these metal powders effected the maximum and critical solid loading of the baseline feedstock formulation. The maximum solid loading using 17-4PH (Atmix) water-atomized powder was 92.5wt% (57vol% metal powder). The maximum solid loading was slightly improved to 92.7wt% (57.6vol% metal powder) by using 17-4PH (UFP) gas-atomized powder with baseline formulation.

2) The gel strength of agar depends on several factors such as type of agar, concentration of agar, and different additives. The gel strength of high concentration (>1wt%) agar gel was improved by about 46% by replacing Meer agar with TIC agar. Increasing the concentration of TIC agar from 0.5 to 3wt% enhanced the gel strength from  $240 \pm 7$  to  $2073 \pm 89$  g/cm<sup>2</sup>. Potassium tetraborate was identified to be the most effective gel-strengthening additive as compared to other borates shown in Table 5.3. The gel strength of 2wt% TIC agar increased from  $1192 \pm 12$  to  $1639 \pm 16$  g/cm<sup>2</sup> by increasing the concentration of potassium tetraborate to more than 0.1wt%.

3) The effect of sucrose, fructose and glucose additives on flowability of the 17-4PH feedstock was evaluated. The addition of sucrose and fructose were ineffective.

Addition of glucose significantly improved the flowability of feedstock made of either gas or water atomized 17-4PH metal powder. Seven different feedstock compositions were evaluated using gas atomized 17-4PH (UFP) powder and the glucose additive. Two compositions were found to be the most effective, composition “G” and “A”. These compositions significantly improved the metal powder loading of the feedstock to 61.7 and 62.5vol% respectively. Representing 4.1 and 5.0vol% improvement in loading compared with the baseline.

4) The effect of these compositions was evaluated with 17-4PH (Atmix) water atomized powder. Both compositions “G<sub>w</sub>” and “A<sub>w</sub>” enhanced the metal powder loading of the feedstock. The maximum solid loading of 59.9 and 60.2vol% was achieved with composition “G<sub>w</sub>” and “A<sub>w</sub>” respectively, Representing 2.9 and 3.2vol% improvement in loading compared with the baseline.

5) A shrinkage prediction model was developed based on conservation of mass and was shown to give predictions in good agreement with data over a range of volume percentage of metal powder loading. The model presents the variation of shrinkage with initial solid loading (vol% of metal powder) and part sinter density.

6) Using the formulations with the glucose additive, significantly reduced the sinter shrinkage. In the case of 17-4PH (Atmix) water atomized powder the reduction shrinkage of 14.756% was obtained by using “A<sub>w</sub>” composition. Baseline shrinkage was 17.15%. Representing a 2.4% improvement in shrinkage minimization. Shrinkage of 13.63% was achieved with using 17-4PH (UFP) gas-atomized powder. Baseline shrinkage was 16.12%.

7) The sintered samples from baseline composition showed an acceptable carbon and oxygen concentrations of 0.008, and 0.044wt% respectively. The carbon and oxygen levels in the sintered samples made with feedstock formulation containing glucose were varied. The final carbon content (0.240 wt%) in composition “G<sub>w</sub>” was higher than specification limit but the oxygen content was (0.012 wt%) within the limit. In the case of composition “A<sub>w</sub>”, the oxygen content (0.38 wt%) is about four times greater than the maximum allowable limits. In contrast its carbon content (0.008 wt%) is in the adequate range. The samples containing glucose additive require additional development of the sintering conditions to obtain the target carbon and oxygen contents.

## 11.2 Future Research

Other related issues for future investigation are:

- 1- The effects of glucose on agar gel strength that contains gel-strengthening additives such as calcium or potassium borates.
- 2- Increasing the critical gelation of agar to higher temperature >40°C. This will drive the molding cycle time to lower values and help to speed up the molding process.
- 3- Studying the effectiveness of formulation “A” and “G” with aluminum oxide ceramic powder and non-ferrous metal powder such as copper alloys.
- 4- Developing a method to measure the as molded green strength of the samples immediately after molding.
- 5- Examining other possible agar/glucose formulations or alternative additives to further reduce the final shrinkage.

## REFERENCES

- [1] E. Gugel, "Net-Shape Processing of Non-Oxide Ceramics" Engineering Applications of Ceramic Materials, American Society for Metals, Ohio, 1985.
- [2] T. Chartier, M. Ferrato, and J. F. Baumard, "Supercritical Debinding of Injection Molding Ceramics" *J. Am. Ceram. Soc.*, 78 (7), 1995, p. 1787-92.
- [3] F. Petzoldt, G. Veltl, and E. D. Kunze, "Investigations of Different Stainless Steel MIM Feedstocks with Novel Binder System" Proceedings, Powder Injection Molding Symposium, The Metal Powder Industries Federation and American Powder Metallurgy Institute, San Francisco, 1992, pp. 155-167.
- [4] C. I. Chung, B. O. Rhee, M. Y. Cao and C. X. Liu, "Requirements of Binder for Powder Injection Molding" Proceedings, Powder Metallurgy Conference and Exhibition, The Metal Powder Industries Federation and American Powder Metallurgy Institute, San Diego, 1989, pp. 67-78.
- [5] M. Y. Cao, J. W. O'Conner and C. I. Chung, "A New Water Soluble Solid Polymer Solution Binder for Powder Injection Molding" Proceedings, Powder Injection Molding Symposium, The Metal Powder Industries Federation and American Powder Metallurgy Institute, San Francisco, 1992, pp. 85-98.
- [6] N. Y. Anwar, H. A. Davies, P. F. Messer and B. Ellis, "Preparation of Feedstock for PIM by Using a New Binder System" *Advances in Powder Metallurgy and Particulate Materials*, 1995, vol. 2, part 6, p. 37-44.
- [7] N. Y. Anwar, H. A. Davies, P. F. Messer and B. Ellis, "A Novel Binder System for Powder Injection Molding" *Advances in Powder Metallurgy and Particulate Materials*, 1995, vol. 2, part 6, p. 15-26.
- [8] Y. Kankawa, K. Saitou, "Injection Molding of SUS316L Powder with Use of Polybutyl-methacrylate and polystyrene" *Journal, Japan Society of Powder And Powder Metallurgy*, 1993, pp. 536-540.
- [9] R. S. Libb, B. R. Paterson, and H. A. Heflin, "Production and Evaluation of PM Injection Molding Feedstock" *Metal Powder Report*, 1988, pp. 255-258.
- [10] J. S. Ebenhoch, "New Binder System for Ceramic Injection Molding" Powder Injection Molding Symposium, MPIF, Princeton, New Jersey, p. 385, 1992.
- [11] M. Bloemacher, D. Weinand, "Injection Molding of Stainless Steel Powders with a New Binder Technique" The Metal Powder Industries Federation and American Powder Metallurgy Institute, San Francisco, 1992, pp. 99-116.

- [12] S. H. Avner, "Introduction to Physical Metallurgy" McGraw-Hill, New York, p.374, 1974.
- [13] I. I. Rubin, "Injection Molding Theory and Practice" John Wiley & Sons, New York, 1972, p. 5.
- [14] R. M. German, "Powder Metallurgy Science" Metal Powder Industries Federation, Princeton, New Jersey, 1994, p. 162.
- [15] R. Aoki, M. Suzuki, "Effect of Particle Shape on the Flow and Packing Properties of Non-Cohesive Granular Materials" Powder Technology, 1970, vol. 4, p.102-104.
- [16] J. S. Reed, "Introduction to the Principles of Ceramic Processing" John Wiley & Sons, New York, 1988, p. 114.
- [17] M. Behi, J. C. LaSalle, "Stable Aqueous Iron Based Feedstock Formulation for Injection Molding" U. S. Patent 6,261,336, 2001.
- [18] The Pharmacopeia of the United State of America, Mack Publishing Co., Easton, Pa. 18<sup>th</sup> Ed., 1970, p. 17.
- [19] H. H. Selbay, R. L. Whistler, "Agar" Industrial Gums, Polysaccharides and Their Derivatives, 3<sup>th</sup> Edition, Academic Press, San Diego, California, 1993, p. 88-89.
- [20] "Guide to Japan's Experts, No. 20, Foreign Trade Press, Tokyo, 1949, p. 1.
- [21] C. K. Tseng, "Colloid Chemistry" J. Alexander, ed., Rheinhold Publishing Corp., New York, vol. 6, 1946, p. 630.
- [22] H. Elsner, Germ. Patent 667,279, 1938; Chem. Abstr. 33,22852, 1939.
- [23] N. H. Larson, Dental Survey, 26, 674, 1950.
- [24] A. J. Fanelli, et al, "Aqueous Process for Injection Molding Ceramic Powders at High Solid Loadings" U. S. Patent 5,250,251, 1993.
- [25] H. H. Selbay, R. L. Whistler, "Agar" Industrial Gums, Polysaccharides and Their Derivatives, 3<sup>th</sup> Edition, Academic Press, San Diego, California, 1993, p. 93.
- [26] M. Behi, J. Burlaw, "Improvement of Flow Characteristics of Stainless Steel Feedstock for Injection Molding" U. S. Patent filed August 2000.
- [27] M. Behi, et al, "Aqueous Injection Molding Binder Composition and Molding Process" U. S. Patent 6,262,150, 2001.

- [28] A. J. Fanelli, M. Behi, "Gel Strength enhancing Additives for Agaroid-Based Binder" U. S. Patent 5,746,957 (1998).
- [29] I. I. Rubin, "Injection Molding Theory and Practice" John Wiley & Sons, New York, 1972, p. 232.
- [30] J. J. Gouza, G. G. Freygang, "Comparison of Spiral-Cavity Mold Flow with Laboratory Scale Tests on Thermoplastics" SEP-J, November 1961, p. 1211.
- [31] R. A. Malloy, "Plastic Part Design for Injection Molding, An Introduction" Hanser Publications, New York, 1994, p. 30.
- [32] R. M. German, A. Bose, "Injection Molding of Metals and Ceramics" Metal Powder Industries Federation, Princeton, New Jersey, 1997, p. 27.
- [33] K. S. Hwang, T. H. Tsou, "Thermal Debinding of Powder Injection Molding Parts: Observations and Mechanisms" Metall. Trans. A., 1992, vol. 23A, p. 2775-82.
- [34] P. Calvert, M. Cima, "Theoretical Models for Binder Burnout" J. Am. Ceram. Sci., 73 (3) 575-79, 1990.
- [35] I. E. Pinwill, M. J. Edirisinghe, M. J. Bevis, "Development of Temperature-Heating Rate Diagrams for the Pyrolytic Removal of Binder Used for Powder Injection Molding" J. Mater. Sci., 22 (1992) 2461.
- [36] K. Okuyama, "Sintering" Powder Technology Handbook, Second Edition, Edited by K. Gotoh, H. Masuda and K. Higashitani, Marcel Dekker, Inc., New York 1997, p. 193.
- [37] D. W. Richerson, "Modern Ceramic Engineering" Second Edition, Marcel Dekker, Inc., New York, 1992, p. 519, 520, 526.
- [38] J. S. Reed, "Introduction to the Principles of Ceramic Processing" John Wiley & Sons, New York, 1988, p. 450.
- [39] W. D. Kingery, H. K. Browen, and D. R. Uhlmann, "Introduction to Ceramics" Second Edition, John Wiley and Sons, 1976, p. 474, 475.
- [40] F. Vollertsen, and M. Geiger, "Precision of P/M Parts: A System Property" Powder Met. Intern. 1990, vol. 22, no. 3, p. 15-20.
- [41] H. E. Exner, G. Petzow, and P. Wellner, "Problems in The Extension of Sintering Theories to Real System" Sintering and Related Phenomena, G. C. Kuczynski, Plenum Press, New York, 1973, p. 351-362.

- [42] Behi M., Fanelli A., “Aluminum Oxide-Based Molding Compound for Injection Molding”, Filed.
- [43] Behi M., Fanelli A., Burlew J., “Process for Forming an Article from Recycled Ceramic Molding Compound”, Patent 6,146,560, November 2000.